



Inhibition of Casein Kinase 2 Protects Oligodendrocytes From Excitotoxicity by Attenuating JNK/p53 Signaling Cascade

Manuel Canedo-Antelo^{1,2,3}, Mari Paz Serrano^{1,2,3}, Andrea Manterola^{1,2,3}, Asier Ruiz^{1,2,3}, Francisco Llavero^{1,4}, Susana Mato^{1,2,3}, José Luis Zugaza^{1,4,5}, Fernando Pérez-Cerdá^{1,2,3}, Carlos Matute^{1,2,3*} and María Victoria Sánchez-Gómez^{1,2,3*}

¹Achucarro Basque Center for Neuroscience, Leioa, Spain, ²Departamento de Neurociencias, Universidad del País Vasco (UPV/EHU), Leioa, Spain, ³Centro de Investigación en Red de Enfermedades Neurodegenerativas (CIBERNED), Leioa, Spain, ⁴Departamento de Genética, Antropología Física y Fisiología Animal, Universidad del País Vasco (UPV/EHU), Leioa, Spain, ⁵IKERBASQUE, Basque Foundation for Science, Bilbao, Spain

OPEN ACCESS

Edited by:

Juan Pablo De Rivero Vaccari,
University of Miami, United States

Reviewed by:

Paul David Morton,
Virginia Tech, United States
Li-Jin Chew,
Children's National Health System,
United States

*Correspondence:

Carlos Matute
carlos.matute@ehu.eus
María Victoria Sánchez-Gómez
vicky.sanchez@ehu.eus

Received: 07 May 2018

Accepted: 27 August 2018

Published: 13 September 2018

Citation:

Canedo-Antelo M, Serrano MP, Manterola A, Ruiz A, Llavero F, Mato S, Zugaza JL, Pérez-Cerdá F, Matute C and Sánchez-Gómez MV (2018) Inhibition of Casein Kinase 2 Protects Oligodendrocytes From Excitotoxicity by Attenuating JNK/p53 Signaling Cascade. *Front. Mol. Neurosci.* 11:333. doi: 10.3389/fnmol.2018.00333

Oligodendrocytes are highly vulnerable to glutamate excitotoxicity, a central mechanism involved in tissue damage in Multiple Sclerosis (MS). Sustained activation of AMPA receptors in rat oligodendrocytes induces cytosolic calcium overload, mitochondrial depolarization, increase of reactive oxygen species, and activation of intracellular pathways resulting in apoptotic cell death. Although many signals driven by excitotoxicity have been identified, some of the key players are still under investigation. Casein kinase 2 (CK2) is a serine/threonine kinase, constitutively expressed in all eukaryotic tissues, involved in cell proliferation, malignant transformation and apoptosis. In this study, we identify CK2 as a critical regulator of oligodendrocytic death pathways and elucidate its role as a signal inductor following excitotoxic insults. We provide evidence that CK2 activity is up-regulated in AMPA-treated oligodendrocytes and CK2 inhibition significantly diminished AMPA receptor-induced oligodendroglial death. In addition, we analyzed mitogen-activated protein kinase (MAPK) signaling after excitotoxic insult. We observed that AMPA receptor activation induced a rapid increase in c-Jun N-terminal kinase (JNK) and p38 phosphorylation that was reduced after CK2 inhibition. Moreover, blocking their phosphorylation, we enhanced oligodendrocyte survival after excitotoxic insult. Finally, we observed that the tumor suppressor p53 is activated during AMPA receptor-induced cell death and, interestingly, down-regulated by JNK or CK2 inhibition. Together, these data indicate that the increase in CK2 activity induced by excitotoxic insults regulates MAPKs, triggers p53 activation and mediates subsequent oligodendroglial loss. Therefore, targeting CK2 may be a useful strategy to prevent oligodendrocyte death in MS and other diseases involving central nervous system (CNS) white matter.

Keywords: CK2, AMPA receptor, oligodendrocyte, apoptosis, mitogen-activated protein kinase (MAPK), c-Jun N-terminal kinase (JNK), p53, excitotoxicity

INTRODUCTION

Glutamate excitotoxic cell death can occur in virtually all cells that express ionotropic glutamate receptors (GluRs) including oligodendrocytes (Yoshioka et al., 1995; Matute et al., 1997; McDonald et al., 1998) and it has been implicated in acute injury to the central nervous system (CNS) and in chronic neurodegenerative disorders (Lipton and Rosenberg, 1994; Choi, 1988; Lee et al., 1999). Oligodendrocytes are particularly vulnerable to glutamate insults through AMPA and kainate receptor-mediated excitotoxicity, a central feature in the pathogenesis of demyelinating disorders such as Multiple Sclerosis (MS; Matute et al., 2007).

Excitotoxic insults to oligodendrocytes are dependent on Ca^{2+} entry through ionotropic GluRs, which alters Ca^{2+} homeostasis and induces changes in the mitochondrial membrane. This mitochondrial dysfunction is mainly mediated by Bax (Sánchez-Gómez et al., 2011; Simonishvili et al., 2013), a proapoptotic member of the Bcl-2 protein, and leads to cytochrome *c* release to the cytosol, where it can activate caspase-9 and downstream caspase-3 and trigger apoptosis (Galluzzi et al., 2009). However, additional proapoptotic signaling pathways initiated by AMPA receptors upstream to mitochondrial dysfunction are relatively unexplored and the involvement of certain molecules that potentially contribute to or oppose the apoptotic cascade still remain unknown.

Protein Casein Kinase 2 (CK2) is a highly conserved serine/threonine kinase present in all tissues, eukaryotic cells and most cellular compartments. CK2 can form a tetrameric structure consisting of two α -subunits with catalytic activity, and two β -subunits that regulate enzymatic activity and substrate specificity (Vilk et al., 1999). The first physiological targets of this kinase were detected in the late 1970s to reach the number of more than 300 in the 2,000 s (Meggio and Pinna, 2003) and it is predictable that proteins phosphorylated by CK2 are much more numerous than those identified to date. Attesting to its importance, changes in CK2 activity are usually associated with significant changes in cell fate. Although the overall function of CK2 is not completely understood, CK2 activity has been associated with many cellular processes including cell cycle progression, differentiation, cell migration, polarity establishment and transformation (Litchfield, 2003; Poole et al., 2005). CK2 activity is a potent and multifunctional promoter of cell growth and survival, and because of that it is currently considered a promising target for cancer therapy (Hanif et al., 2010; Pierre et al., 2011). Nonetheless, in contrast to the evidence that CK2 functions as a cell survival mediator, several studies have described a proapoptotic contribution for this enzyme specifically linked to c-Jun N-terminal kinase (JNK) activation (Min et al., 2003; Hilgard et al., 2004). In addition to its apoptotic function, a number of studies have suggested a pro-inflammatory role for CK2, including investigations using experimental autoimmune encephalomyelitis (EAE), a key animal model for MS. These studies established that the CD5-dependent CK2 signaling pathway represents a major signaling cascade initiated by CD5 that regulates the threshold of T cell activation and Th differentiation and impacts the outcome

of EAE, so that mice deficient in CD5-CK2 signaling pathway are mostly resistant to EAE (Axtell et al., 2006; Sestero et al., 2012; Mier-Aguilar et al., 2016). In addition, CK2 pharmacological inhibition ameliorates EAE severity and relapse incidence (Ulges et al., 2016) as well as attenuates apoptosis and inflammatory cell infiltration after renal ischemia-reperfusion injury (Ka et al., 2015).

Given that apoptosis and inflammation are critical events for MS, CK2 activation may have some role in the pathogenesis of MS not only restricted to pro-inflammatory events but also in apoptotic cascade induced by concomitant excitotoxic context. However, it is unknown whether CK2 is involved in the vulnerability of oligodendrocytes during excitotoxic insults. In the present study, we investigated the possible role of CK2 in this deleterious process and its potential relationship with other molecular effectors of death.

MATERIALS AND METHODS

Ethics Statement

This study was carried out in accordance with the recommendations and the approval of the internal animal ethics committee of the University of the Basque Country (UPV/EHU), in accordance with the European Communities Council Directive. All the protocols were approved by the “Ethics Committee on Animal Experimentation (CEEAA)” which is a collegiate authority into the operational structure of the Ethics Commission for Research and Teaching (CEID) of the University of the Basque Country. The committee CEEAA is also authorized by the Ministry of Science and Innovation to evaluate projects that experiment with animals. All possible efforts were made to minimize animal suffering and the number of animals used. Rats and mice in both sexes were used for all experiments.

Oligodendrocyte Culture

Highly enriched OPCs were prepared from mixed glial cultures obtained from newborn (P0–P2) Sprague–Dawley rat forebrain cortices as previously described (McCarthy and de Vellis, 1980) with minor modifications (Chen et al., 2007; Bernal-Chico et al., 2015). Briefly, forebrains were removed from the skulls and the cortices isolated and enzymatically digested by incubation with 0.25% trypsin and 4% DNase for 15 min at 37°C. Then, the tissue was mechanically dissociated and plated in Iscove’s Modified Dulbecco’s Medium (IMDM) supplemented with 10% fetal bovine serum (FBS, Hyclone). The mixed glial cells were grown in T75 flasks (pre-treated with poly-d-lysine) until they were confluent (10–12 days). Microglia were separated from the cultures by shaking the flasks on a rotary shaker for 1 h at 250 revolutions/min. OPCs were isolated following an additional 18 h. OPCs were seeded on to poly-d-lysine-coated coverslips and were maintained at 37°C and 5% CO₂ for 2 days in a chemically defined proliferation medium SATO composed of: 100 μ g/ml BSA, 100 μ g/ml transferrin, 16 μ g/ml putrescine, 60 ng/ml progesterone, 40 ng/ml selenium, 6.3 mg/ml N-acetyl-cysteine, 0.5 mg/ml insulin (all of from Sigma) and growth factors b-FGF (5 ng/ml) and PDGF-AA (5 ng/ml; from

PeproTech) to amplify the number of oligodendroglial cells. These conditions produced cultures that contain $95 \pm 0.2\%$ Olig2+, $92.5 \pm 0.5\%$ PDGF-R α + oligodendroglial cells, and $1.4 \pm 0.3\%$ GFAP+ astrocytes and $2.4 \pm 0.5\%$ Iba1+ microglia. After the proliferation stage, medium was replaced with maturation SATO composed by 100 μ g/ml BSA, 100 μ g/ml transferrin, 16 μ g/ml putrescine, 40 ng/ml thyroxine, 30 ng/ml tri-iodothyronine, 60 ng/ml progesterone, 40 ng/ml selenium, 6.3 mg/ml N-acetyl-cysteine, 0.5 mg/ml insulin (all from Sigma), plus 1 μ g/ml CNTF and 10 μ g/ml NT3 (both from PeproTech) to induce oligodendrocyte maturation. Cells were used 2 days later for different experiments whose common point is the treatment with 10 μ M AMPA plus 100 μ M cyclothiazide (CTZ; added 5 min before AMPA) for 30 min to recreate AMPA-induced excitotoxic conditions (Sánchez-Gómez and Matute, 1999).

In vitro CK2 Kinase Assay

Oligodendrocytes were incubated in the absence or presence of CK2 inhibitor (TBB; 5 μ M for 3 h) or CK2 activator (spermine; 10 μ M for 1 h), and then treated with 10 μ M AMPA plus CTZ for 30 min. Thereafter, cells were washed twice with cold phosphate-buffered saline (PBS), lysed with lysis buffer (20 mM Tris, pH 7.4, 137 mM NaCl, 5 mM EDTA, 1 mM EGTA, 10 mM NaF, 1 mM sodium pyrophosphate, 100 μ M β -glycerophosphate, 10 μ g/ml of aprotinin, 1 mM PMSF, 10% glycerol, and 1% (v/v) Triton X-100) and lysates were clarified by centrifugation at 12,300 g for 10 min at 4°C. Supernatants were recollected and subjected to CK2 α immunoprecipitation by the addition of CK2 α specific antibody (1:500; Santa Cruz Technologies) and the immunocomplex formed were captured by incubation with Gamma Bind Plus-Sepharose beads (GE Healthcare) for 4 h with gentle rotation at 4°C. Then, the mix was centrifuged at 400 g for 1 min and the supernatants were discarded. The beads were washed twice with cold lysis buffer, twice with cold washing buffer (10 mM HEPES, pH 7.4, 100 mM NaCl, 20 μ g/ml of aprotinin, and 0.5% IGEPAL-360) and resuspended in reaction buffer (20 mM Tris, pH 7.4, 20 mM NaCl, 1 mM DTT, 10 mM MgCl₂, and 1 mM MnCl₂). Then, 40 μ l of each sample were assayed for *in vitro* kinase reaction in the presence of 500 ng of purified recombinant GST-RCAN3 (generous gift from Dr. Mercé Pérez-Riba), which represent a potential serine phosphorylation target of CK2 (Martínez-Hoyer et al., 2013), and 200 μ M ATP. The reaction was carried out for 30 min at 30°C and stopped by adding 30 μ l of 2 \times loading buffer. The samples were boiled and resolved by SDS-PAGE and immunoblotting using a mouse anti-phosphoserine antibody (anti-pSerine; 1:1,000; Sigma Aldrich), a rabbit anti-GST antibody (1:5,000; Abcam) or a rabbit anti-CK2 α (1:500; Sta. Cruz Technologies) and enhanced chemiluminescence detection kit, according to the manufacturer's instructions (Supersignal; Thermo Scientific). In addition, western blotting against CK2 α was developed in whole cell lysate to confirm that equivalent amounts of CK2 α were present in all samples.

Quantitative PCR

Total RNA was extracted from cell cultures with TRIzol reagent according to the manufacturer's recommendations

(Invitrogen, Barcelona, Spain). First strand cDNA synthesis was performed with reverse transcriptase SuperScriptTM III (Invitrogen) using random primers as previously described (González-Fernández et al., 2014). Specific primers for CK2 α , CK2 β , MDM2 and PUMA were designed with the PrimerExpress software (Applied Biosystems) and were targeted to exon junctions to avoid amplification of contaminating genomic DNA. Primers sequences were as follows: rat CK2 α forward TGGTGGAATGGGGAAATCAAG and reverse CCTGCCTAATTTT CGAACAAAGC; rat CK2 β forward GGACCTGGAACC TGATGAAGAG and reverse TTTCCAACATTTGTGCAATGC; rat MDM2 forward AGGATGATGAGGTCTATCGGGTC and reverse GAGGATTCATTTTCATTGCACGA; rat PUMA forward CAGTGCGCCTTCACTTTGG and reverse GGGTTGAGAAG GCTTTCACATG.

Real-time quantitative PCR (qPCR) was performed using SsoFastTM EvaGreen Supermix (Bio-Rad, Barcelona, Spain). Amplifications were run in a CFX96TM Real Time System (Bio-Rad). Each value was normalized against GADPH and HPRT levels as endogenous reference and relative gene expression data were determined by the $2^{-\Delta\Delta Ct}$ method.

Toxicity Assays

Toxicity assays were performed as described previously (Sánchez-Gómez et al., 2003), with minor modifications. Oligodendrocytes, after 2 days in maturation medium, were exposed to 100 μ M CTZ for 5 min before incubation with 10 μ M AMPA for 30 min. The medium was subsequently removed and the cells incubated overnight in AMPA-free fresh medium. For studies with the different activator or inhibitors, cells were pretreated with the dilution and for the time indicated for each drug before the incubation with CTZ/AMPA, and all drugs were present during stimulus application. These compounds used were: CK2 activator spermine; CK2 inhibitors TBB, DRB and resofurin; JNK inhibitor SP600125; p38 inhibitor PH79804 and p53 inhibitors pifithrin- α and pifithrin- μ . Oligodendrocyte viability was assessed 24 h later by loading cells with 1 μ M calcein-AM (Molecular Probes; Invitrogen; C3100) for 30 min and fluorescence was measured using a Synergy-HT fluorimeter (Bio-Tek Instruments Inc., Winooski, VT, USA) as indicated by the supplier (485 nm excitation wavelength and 530 nm emission wavelength). All experiments were performed in duplicate, and the values provided here are the averages of at least three independent experiments.

Immunocytochemistry

Oligodendrocytes were obtained from mixed glial cultures and treated for AMPA receptor activation as described above. Following treatments, cells were rinsed in PBS and fixed in 4% paraformaldehyde in PBS for 20 min at room temperature, permeabilized in 0.1% Triton X-100 in PBS and processed for immunofluorescence with rabbit anti-CK2 α (1:100; Santa Cruz Technologies), anti-total p53 (FL-393; 1:100; Santa Cruz Technologies) or anti-phospho-p53 (Ser15; 1:100; Cell Signaling) and anti-COX-IV (1:200; Cell Signaling) in experiments in which mitochondria were stained. Primary antibodies were detected after incubation with anti-rabbit IgG (H+L) Alexa Fluor-488

or Alexa Fluor-594 (1:200; Invitrogen) secondary antibody, for 2 h at room temperature. Incubation for 10 min with DAPI (1:1,000) was used, when required, to identify nuclei. Cells were washed three times in PBS, mounted on slides with Glycergel (Dako, Glostrup, Denmark), and visualized with a laser scanning confocal microscope (Olympus Fluoview FV500) at the Analytic and High Resolution Microscopy Facility in the University of the Basque Country. No staining was detected in control samples run in parallel without primary antibodies.

Measurement of Intracellular Reactive Oxygen Species

Accumulation of reactive oxygen species within cells was measured, as previously described (Sánchez-Gómez et al., 2011) by loading cells with 10 μ M of the oxidation-sensitive fluorescent dye 5-(and-6)-chloromethyl-2',7'-dichlorodihydrofluorescein diacetate (CM-DCFDA; Molecular Probes, Invitrogen; C6827), for 20 min at 37°C, 5% CO₂, using 1 μ M calcein-AM as a control dye. Fluorescence was measured using a Synergy-HT fluorimeter (Bio-Tek Instruments Inc., Winooski, VT, USA) and data were expressed as a normalized percentage of CM-DCFDA/calcein fluorescence in controls (untreated oligodendrocytes; 100%). Excitation and emission wavelengths for CM-DCFDA were 488 and 515 nm, respectively. All assays were performed in duplicate and the values are the average of at least three independent experiments (mean \pm SEM).

Analysis of Mitochondrial Membrane Potential

Oligodendrocyte cultures were exposed to AMPA alone or in presence of different drugs and changes in mitochondrial membrane potential were monitored by reduction of 5, 5',6,6'-tetrachloro-1,1',3,3'-tetraethylbenzimidazolcarbocyanine iodide (JC-1; Invitrogen), according to the manufacturer's protocol. Briefly, after drug treatment, cells were loaded with 3 μ M JC-1 in culture medium for 15 min at 37°C and were washed with HBSS without phenol red two times to eliminate the excess of dye. In the cytosol the monomeric form of this dye fluoresces green (emission read at 529 nm when excited at 485 nm), whereas within the mitochondrial matrix highly concentrated JC-1 forms aggregates fluoresces red (emission at 590 nm when excited at 485 nm). Both JC-1 monomers and aggregates were detectable using a Synergy-HT fluorimeter (Biotek Instruments) and the changes in mitochondrial potential were calculated as the red/green ratio for each condition. The data were expressed as a normalized percentage of fluorescence in controls (untreated cells; 100%). All experiments ($n \geq 3$) were performed at least in triplicate and plotted as mean \pm SEM.

Western Blotting Analysis

Total protein from rat oligodendrocytes (2×10^5 cells) was obtained at specific time points after the drug treatment by washed with ice-cold PBS and then collected by mechanical scraping with 50 μ l of RIPA buffer (50 mM Tris, pH 7.5, 150 mM NaCl, 0.5% Na-desoxycolate, 0.1% SDS, 1% NP-40, 1 mM EDTA) supplemented with HaltTM protease and phosphatase

inhibitor cocktail (Thermo Fisher Scientific, Spain). Lysates were boiled in sample buffer for 5 min, and separated by electrophoresis using Criterion TGX Precast 12% gels and transferred to Trans-Blot Turbo Midi PVDF Transfer Packs (Bio-Rad, Hercules, CA, USA). After electroblotting on PVDF membranes (Bio-Rad), these were blocked in 5% skimmed milk, 5% serum in TBST for 1 h. The blots were probed with primary antibodies in 5% BSA in TBST: rabbit anti-CK2 α (1:500; Santa Cruz Technologies); rabbit anti-phospho-JNK (1:1,000; Cell Signaling); rabbit anti-JNK (1:1,000; Cell Signaling); rabbit anti-phospho-p38 (1:1,000; Cell Signaling); rabbit anti-p38 (1:1,000; Cell Signaling); mouse anti-total p53 (1C12; 1:500; Cell Signaling); rabbit anti-PUMA (1:1,000; Cell Signaling); rabbit anti-phospho-p53 (Ser15; 1:1,000; Cell Signaling); rabbit anti-actin (1:5,000; Sigma) overnight at 4°C. After washing, the blots were developed using HRP-conjugated anti-IgG (1:5,000) and an enhanced chemiluminescence detection kit, according to the manufacturer's instructions (Supersignal; Thermo Scientific). Images were acquired with a ChemiDoc MP system (BioRad) and quantified with ImageJ software.

AMPA Receptor Activation in Isolated Mice Optic Nerves

Transgenic mice PLP-DsRed, generous gift from Dr. Frank Kirchhoff (University of Saarland, Homburg, Germany), were used in which fluorescent reporter DsRed was under control of the glial-specific promoter proteolipid protein (PLP; Hirrlinger et al., 2005). Optic nerves from P25 PLP-DsRed mice were dissected out in cold oxygen-saturated artificial CSF containing 126 mM NaCl, 3 mM KCl, 2 mM MgSO₄, 26 mM NaHCO₃, 1.25 mM NaH₂PO₄, 2 mM CaCl₂ and 10 mM glucose and were freed from of their meninges, as previously described (Sánchez-Gómez et al., 2003). Subsequently, nerves were placed in a 48-well plate containing artificial CSF and pre-incubated with 25 μ M TBB for 3 h or 20 μ M SP600125 for 1 h, at 37°C and 5% CO₂, and then treated with 100 μ M CTZ for 15 min before addition of AMPA (100 μ M; 2 h). Following incubation, media was replaced with fresh oxygen-saturated artificial CSF and incubated for another 90 min at 37°C. Tissue damage was analyzed by measuring lactate dehydrogenase (LDH) release in the incubation media at 30, 60 and 90 min post-stimulus, using the CytoTox 96[®] assay (Promega Biotech Ibérica, Spain). At the end of LDH evaluation time course and to monitor tissue damage by histology, optic nerves were fixed for 1 h in 4% paraformaldehyde, washed in PBS and mounted on glass slides with Prolong[®] Gold antifade mounting media (Invitrogen; Molecular Probes) and sealed with coverslips. Images were acquired using a laser scanning confocal microscope (Olympus Fluoview FV500) at the Analytic and High Resolution Microscopy Facility in the University of the Basque Country, with a 10 \times objective. The number of z-sections were optimized with FluoView software, sections were <0.75 μ m thickness, and approximately 15 z-sections for each optic nerve, until analyzing it completely. The fluorescence signal corresponding to the PLP-DsRed⁺ oligodendrocytes that were present in the images was quantified by ImageJ software and the data were expressed as arbitrary units of fluorescence for each experimental situation.

Cell counts of PLP-DsRed⁺ oligodendrocytes in intact optic nerves were performed on flattened confocal z-stacks of 15 μm thickness, taken with a 20 \times objective along the entire nerve, with a field of view (FOV) volume of $6 \times 10^6 \mu\text{m}^3$ (based in Azim and Butt, 2011). Cells expressing DsRed fluorochrome within this area were counted using the ImageJ “Cell Counter” plugin and the results were represented as mean \pm SEM cells per FOV ($n \geq 4$), where n represents number of mice in each experimental condition.

To analyze oligodendrocyte cell death, immunohistochemistry was performed and damage was determined by imaging and DAPI labeling. After treatments, nerves were fixed for 2 h in 4% PFA, in 0.1 M sodium phosphate buffer, cryoprotected in 15% sucrose and frozen. Cryostat sections (10 μm) were mounted onto glass slides and processed for immunofluorescence with rabbit antibodies to APC (Ab-7; 1:200, Calbiochem), specific marker for oligodendrocytes, and fluorescein-conjugated anti-rabbit (1:200; Alexa Fluor 488; Molecular Probes). The sections were incubated with DAPI (1:1,000) for nuclear staining and processed for viewing under confocal microscope as indicated above.

Gene Silencing Procedures

SureSilencing shRNA Plasmids (Sh-CK2; Csnk2a1 SureSilencing shRNA Plasmid (KR43385) and control negative Sh-Scrambled; Qiagen) were first amplified into competent *E. coli* cells. Growing colonies were picked for large-scale bacterial culture and then plasmids were purified using Maxiprep Kit (PureLink[®] HiPure Plasmid Filter Maxiprep Kit; Invitrogen).

Rat oligodendrocytes (1.5×10^6 cells) were transfected in suspension with gene-specific (Sh-CK2 α) and negative control (Sh-Scrambled) shRNA plasmids, both of them including a puromycin resistance gene. Transfection was carried out using Rat Glial Nucleofector Kit (Lonza, Basel, Switzerland) according to the manufacturer instructions, and cells were immediately plated and maintained in maturation medium, as described above. Following transfection, cells were replated 16–18 h into SATO medium containing puromycin (0.3 $\mu\text{g}/\text{ml}$) to begin the process of selecting for and cloning stably transfected cells. One day after the withdrawal of the puromycin, transfected oligodendrocytes were exposed to usual excitotoxic conditions, 100 μM CTZ for 5 min before incubation with 10 μM AMPA for 30 min, and toxicity assays or western blot (WB) analysis were carried out as described above to non-transfected oligodendrocytes experiments.

Immunoprecipitation Assay

Oligodendrocyte cultures were treated in the absence (control) or presence of 100 μM CTZ and 10 μM AMPA for 30 min. Cells were washed three times in ice-cold PBS and lysed in RIPA buffer at different times (30, 60 or 90 min) after AMPA receptor activation. Lysates were pre-cleared with Sepharose 6B (Sigma-Aldrich) for 1 h at 4°C with a rotating wheel and then immunoprecipitated overnight at 4°C with Protein A-Sepharose beads (Abcam) previously bound with rabbit anti-CK2 α (Santa Cruz Technologies) or mouse anti-p53 (1C12; Cell Signaling) antibody. Beads were then washed three times

with 1 \times lysis buffer, and immunoprecipitates were eluted with SDS gel loading buffer, boiled for 5 min and processed for immunoblotting for detection of p53 (using the mouse anti-p53) or phospho-p53 in Ser15 (using the rabbit anti-phospho-p53 (Ser15)), respectively. Total CK2 α , p53 and β -actin were used as loading controls in whole cell lysate in the different situations. Immunoreactive bands were visualized using enhanced chemiluminescence detection kit, according to the manufacturer’s instructions (Supersignal; Thermo Scientific).

Statistical Analysis

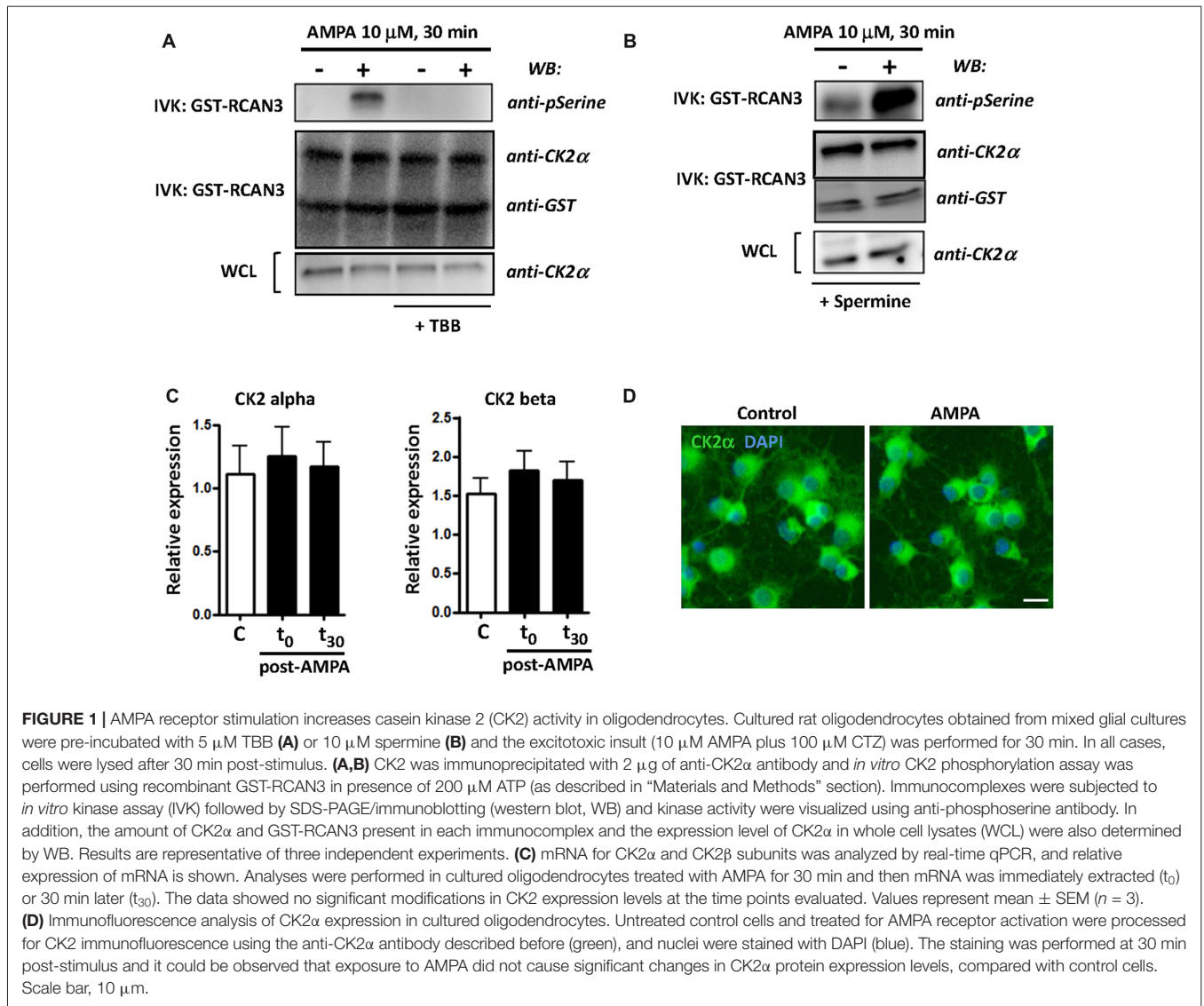
The analyzed number of samples was described in each experiment. All data are shown as mean \pm SEM. Statistical analyses were performed using GraphPad Prism statistical software (version 5.0; GraphPad Software). Comparisons between multiple experimental groups were made using one-way ANOVA with Tukey’s *post hoc* test. For comparisons between a single experimental group and a control group, we used two-tailed Student’s *t*-test assuming equal variance. Statistical differences were considered significant where $p < 0.05$. All the images shown in this article represent the data obtained, at least, in three independent experiments with similar results.

RESULTS

AMPA Receptor Stimulation Increases CK2 Activity in Oligodendrocytes

CK2 kinase activity is increased in some cellular stress conditions and this has deep consequences in cell viability (Sayed et al., 2001; Manni et al., 2012). To further define CK2 function in oligodendroglial death in AMPA receptor-induced excitotoxic events, we analyzed the activation of catalytic subunit CK2 α and the expression of both catalytic and regulatory subunits of CK2 (CK2 α and CK2 β) under different experimental conditions. First, we carried out an *in vitro* kinase assay to examine the activity of CK2 α (hereafter referred to as CK2) in oligodendrocytes after AMPA receptor stimulation (10 mM, 30 min) in the absence or in the presence of CK2 inhibitor TBB (5 mM; 3 h pre-treatment) or CK2 activator spermine (10 mM; 1 h pre-treatment). The kinase activity, determined by WB using an anti-phosphoserine antibody, showed that AMPA receptor stimulation induced potent increase of CK2 activity and this effect was not detected in the presence of TBB (Figure 1A). On the other hand, as expected, when oligodendrocytes were pretreated with CK2 activator spermine, AMPA-induced increase in CK2 activity was higher compared to that observed in cells treated only with agonist (Figure 1B). In addition, we also determined by WB the protein level of CK2 α and GST-RCAN3 present in each immunocomplex as well as CK2 α in whole cell lysates (WCL) what revealed similar amounts of these proteins in all the samples analyzed.

Additionally, and to determine whether AMPA-induced CK2 activity was correlated with modifications in the mRNA expression of catalytic and/or regulatory CK2 subunits we analyzed by RT-PCR their expression level in oligodendrocytes treated with AMPA (10 mM; 30 min) and evaluated immediately after treatment ($t = 0$) and 30 min later ($t = 30$). Consistent



with immunoblot findings, we observed that CK2 subunits was constitutively expressed in oligodendrocytes but that their expression levels were not significantly increased after AMPA stimulation at the time points analyzed (Figure 1C). Similar results were obtained through immunofluorescence analysis on cultured oligodendrocytes, control and exposed to AMPA, using the anti-CK2 α antibody (Figure 1D).

Taken together, these results indicate that AMPA excitotoxic insults in oligodendrocytes provoke a potent increase in CK2 kinase activity without causing significant changes in the CK2 mRNA or protein levels.

CK2 Inhibition Rescues Cultured Oligodendrocytes From AMPA-Induced Excitotoxic Death

We have previously determined that rat oligodendrocytes are highly vulnerable to excitotoxic signals induced by

overstimulation of AMPA receptors and that this toxicity is mediated by apoptotic mechanisms involving calcium overload, mitochondrial dysfunction, as well as activation of Bax, calpain and caspase -8, -9 and -3 (Sánchez-Gómez et al., 2003, 2011). Here, we investigated whether CK2, an enzyme closely linked with cell fate and whose activity we observed increased after AMPA treatment, contributes to oligodendroglial apoptotic program triggered by this glutamatergic agonist. To provide evidence that CK2 influences cellular viability, we induced AMPA receptor activation in oligodendrocytes in absence or presence of CK2 inhibitors and observed that cell death was significantly reduced when CK2 was inhibited (Figure 2A). So, activation of AMPA receptors with 10 mM AMPA, applied together with 100 mM CTZ for 30 min, caused oligodendroglial cell death ($18.0 \pm 3.9\%$), while oligodendrocytes treated previously with CK2 inhibitors (TBB, DRB or resorufin) were more resistant to these insults ($7.9 \pm 4.1\%$; $6.3 \pm 3.4\%$ and $5.7 \pm 3.7\%$, respectively; Figure 2A). On the other hand, the

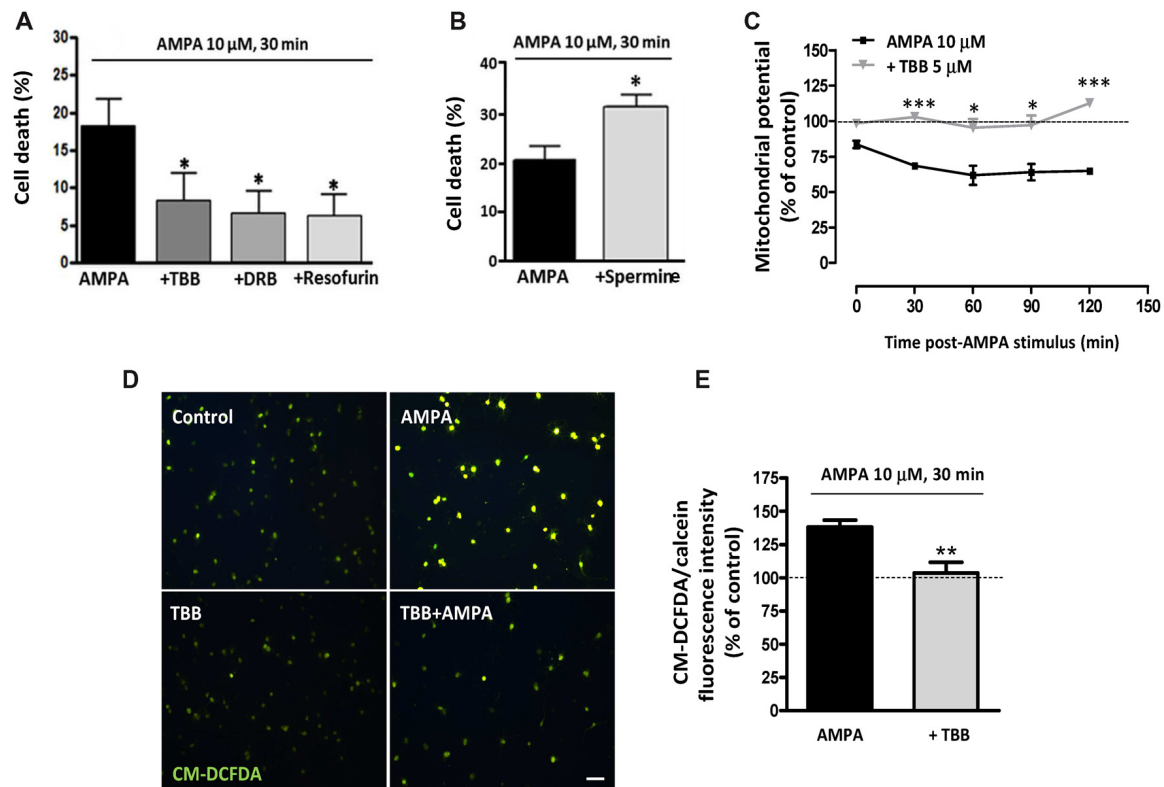


FIGURE 2 | CK2 inhibition protects rat oligodendrocytes from AMPA excitotoxic insults. Oligodendrocyte cultures were isolated from mixed glial culture and used for toxicity assays after 2 days *in vitro* in differentiation SATO medium. **(A)** Activation of AMPA receptors with 10 μM AMPA applied together with 100 μM cyclothiazide for 30 min, caused oligodendroglial cell death as measured by calcein-AM assay 24 h later. AMPA-induced cytotoxicity was significantly reduced in presence of CK2 inhibitors, 5 μM TBB, 5 μM DRB or 5 μM resofurin and none of these CK2 inhibitors produced alterations in the oligodendrocyte viability when they were used without AMPA (data not shown). The data are shown as mean \pm SEM ($n \geq 4$; $*p < 0.05$ compared with cells treated with AMPA). **(B)** Pretreatment of cells with CK2 activator spermine (10 μM) increased cytotoxic consequences derived from AMPA receptor activation in oligodendrocytes. Bars represent mean \pm SEM ($n \geq 3$; $*p < 0.05$ compared with cells treated with AMPA). **(C)** CK2 inhibitor TBB attenuated loss of mitochondrial membrane potential induced by activation of AMPA receptors. Oligodendrocytes were exposed to 10 μM AMPA for 30 min in absence or presence of TBB (5 μM ; 3 h pretreatment) and mitochondrial membrane potential was quantified by fluorimetry at the indicated times post-AMPA stimulus, after loading cells with dye JC-1 (3 μM , Molecular Probes). Decrease of mitochondrial potential triggered by excitotoxic insult was not observed in oligodendrocytes pretreated with 5 μM TBB. The data are represented as mean \pm SEM compared with untreated control cells for each time point analyzed ($n \geq 4$; $*p < 0.05$, $***p < 0.001$). **(D,E)** ROS generation induced by activation of AMPA receptors was limited in the presence of CK2 inhibitor TBB. Oligodendrocytes were treated similarly as described above and ROS generation was determined immediately afterwards using the dye CM-DCFDA (10 μM , Molecular Probes). Cells were observed under fluorescence microscopy **(D)** and quantification of signal was measured using a Synergy-HT fluorimeter **(E)**. Histogram shows that levels of ROS induced by AMPA were attenuated in oligodendrocytes pretreated with TBB. Data represent mean \pm SEM ($n = 3$; $**p < 0.01$, compared with cells treated only with agonist).

presence of CK2 activator spermine increased almost twice AMPA-induced oligodendrocyte cell death ($31.4 \pm 2.6\%$), as shown in **Figure 2B**.

The above results provide evidence that CK2 is involved in excitotoxic insults. Since mitochondrial dysfunction is pivotal to this type of injury, we next analyzed whether CK2 also participate in the mitochondrial alterations that occur during oligodendrocyte excitotoxicity. Then, we determined mitochondrial depolarization and ROS production triggered by AMPA exposure (10 μM , in conjunction with 100 μM CTZ; 30 min) in absence or presence of CK2 inhibitor TBB (5 μM ; 3 h pretreatment). We evaluated the mitochondrial membrane potential in these oligodendrocyte cultures, using the fluorescent probe JC-1, and performed its quantification at different times post-stimulus (**Figure 2C**). Consistent with the toxicity assays,

we found that mitochondrial membrane depolarization resulting from those excitotoxic insults was attenuated in the presence of CK2 inhibitor TBB so that oligodendrocytes pretreated with TBB showed mitochondrial membrane integrity similar to the detected in untreated control cells, at all times analyzed (**Figure 2C**). Finally, cells subjected to excitotoxic stimulus were loaded with the probe CM-DCFDA for ROS detection and we observed that ROS generation triggered by AMPA receptor activation (up to $138.8 \pm 4.4\%$) was significantly reduced in the presence of CK2 inhibitor TBB ($103.7 \pm 8.1\%$; **Figures 2D,E**).

Overall, these results indicate that pharmacological CK2 inhibition reduces both cell death as well as loss of mitochondrial membrane potential and acute generation of reactive oxygen species associated with AMPA-caused excitotoxicity in oligodendrocytes *in vitro*.

Proapoptotic Contribution of CK2 Is Associated With MAPKs Activation Triggered by AMPA in Oligodendrocytes

Although some studies have described that CK2 may protect against cell death in different contexts (Ahmad et al., 2008; Turowec et al., 2010) other works indicated that, under certain cell-specific conditions, CK2 can act as pro-death molecule, for instance, via CK2-JNK interaction (Min et al., 2003; Hilgard et al., 2004; Ka et al., 2015). With this premise, we tried to define the mechanism by which CK2 inhibition rescues oligodendrocytes from excitotoxic death and, specifically, if mitogen-activated protein kinase (MAPK)s activated by stress JNK and p38 are part of this pathway. For that, we first examined, by WB with specific antibodies, the phosphorylation (activation) state of JNK and p38 in total cell lysates obtained from control and AMPA-exposed oligodendrocytes. As depicted in **Figure 3**, phosphorylation levels of both enzymes were early and robustly induced after agonist exposure, reaching values for phospho-JNK of $505.3 \pm 28.2\%$; $352.4 \pm 20.6\%$; $332.0 \pm 17.4\%$ and $167.0 \pm 17.3\%$ at 10, 30, 60 and 120 min post-stimulus, respectively, and for phospho-p38 of $314.9 \pm 16.4\%$; $438.3 \pm 25.5\%$; $471.7 \pm 22.7\%$ and $310.4 \pm 27.3\%$ at the same times analyzed, always compared to untreated control cells (100%; **Figure 3A**). The presence of inhibitor of JNK SP600125 significantly reduced AMPA-induced JNK activation ($108.1 \pm 11.9\%$ and $118.2 \pm 10.5\%$ compared with $451.0 \pm 31.4\%$ and $288.3 \pm 39.36\%$ observed in AMPA-treated cells without inhibitor, at 10 and 30 min after stimulus, respectively; **Figure 3B**). Similarly, the activation/phosphorylation of p38 triggered by AMPA was significantly reduced when its inhibitor PH797804 was present during the treatment (**Figure 3D**). This reduction of phosphorylation levels, both JNK and p38, supported the effectiveness of these inhibitors in the conditions used, so we used them in the following assays.

It should be mentioned that the potent and fast induction of JNK and p38 activation is consistent with their role as members of death signaling axis, triggered by toxic signals and mediating in the activation of downstream apoptotic molecules. In order to check the involvement of JNK and/or p38 in the apoptotic process triggered by AMPA in oligodendrocytes, we developed toxicity assays in the presence of their specific inhibitors, SP600125 and PH797804, respectively. As we showed in **Figures 3C,E** the oligodendroglial death caused by AMPA exposure (10 μ M; 30 min) was significantly reduced in the presence of each inhibitor. So, the values of cell death were of $5.3 \pm 1.2\%$ in presence of SP600125, compared with $18.2 \pm 2.0\%$ for cells only treated with AMPA (**Figure 3C**) and $2.6 \pm 2.2\%$ in presence of PH797804, compared to $10.8 \pm 2.4\%$ in absence of this inhibitor (**Figure 3E**).

Then, and to determine the possible relationship between CK2 and JNK/p38 axis after AMPA receptor stimulation in oligodendrocytes, we determined the phosphorylation state of both kinases in AMPA treated cells in absence or presence of CK2 inhibitor TBB (**Figure 3F**). We found that AMPA-induced phosphorylation of JNK ($403.2 \pm 29.7\%$; $299.3 \pm 38.7\%$ at 10 and

30 min after stimulus, respectively) and p38 ($324.3 \pm 23.1\%$; $361.0 \pm 22.6\%$ at the same time post-stimulus), was significantly reduced in TBB pre-treated oligodendrocytes ($122.5 \pm 16.5\%$; $116.7 \pm 8.5\%$ for phospho-JNK and $164.7 \pm 10.5\%$; $181.7 \pm 7.7\%$ for phospho-p38 at the times indicated, respectively).

These results indicate that TBB, inhibitor of CK2, regulates the MAPK signaling pathway induced by AMPA in oligodendrocytes, so that the level of phosphorylation of JNK and p38 depends on the degree of activation of CK2. This molecular interaction could have important implications in the resistance/vulnerability of the oligodendrocytes subjected to excitotoxic conditions.

CK2-JNK Are Involved in AMPA-Caused Damage Oligodendrocyte in Isolated Optic Nerves

To further investigate the deleterious effects of AMPA in a more integral preparation, we analyzed the AMPA receptor-mediated injury to intact optic nerves, a preparation which we have previously used to test receptor-mediated toxicity (Sánchez-Gómez et al., 2003; Domercq et al., 2010; Mato et al., 2013; González-Fernández et al., 2014). In this case, we used isolated intact optic nerves from transgenic mice (PLP-DsRed) which allows identification of the soma and the processes of oligodendrocytes by red fluorescence. Freshly isolated optic nerves from P25 mice were exposed for 2 h to AMPA plus CTZ (100 μ M each) in oxygen-saturated artificial CSF, in presence or absence of inhibitors TBB or SP600125 and cell damage was monitored by measuring LDH release at 30, 60 and 90 min after the withdrawal of the stimuli (**Figures 4A,B**). Incubation of optic nerves with the agonist induced a marked damage that was increasing over time after AMPA exposure, reaching values for LDH release 90 min later, up to near four times higher than the control ($369.1 \pm 35.2\%$ respect to 100% control). This harmful effect was absent when nerves were preincubated with CK2 inhibitor (TBB; 25 μ M, 3 h; **Figure 4A**) or with JNK inhibitor (SP600125; 20 μ M, 1 h; **Figure 4B**) and maintained 2 h with AMPA stimulus in the incubation medium. The protective effect of both inhibitors was statistically significant at all times post-stimulus analyzed, included at 90 min after removal of the agonist (**Figures 4A,B**).

Additionally and when LDH release assays were completed, optic nerves were fixed and high-resolution confocal z-sections of whole-mounted nerves were obtained. As showed in representative images of optic nerves, the incubation of isolated intact optic nerves with AMPA induced a potent loss of oligodendrocytes and their processes (**Figure 4C**), which was prevented in the presence of TBB or SP600125 (**Figure 4D**). The quantification of fluorescent signal in the z-stacks of whole nerves corroborated this effect, and showed that the disappearance of the half of DsRed fluorescent caused by AMPA (arbitrary units 0.10 ± 0.01 respect to 0.21 ± 0.01 of control) was abolished when the inhibitors were added (arbitrary units 0.19 ± 0.02 for TBB and 0.19 ± 0.04 for SP600125; **Figure 4E**). In addition, we counted individually the

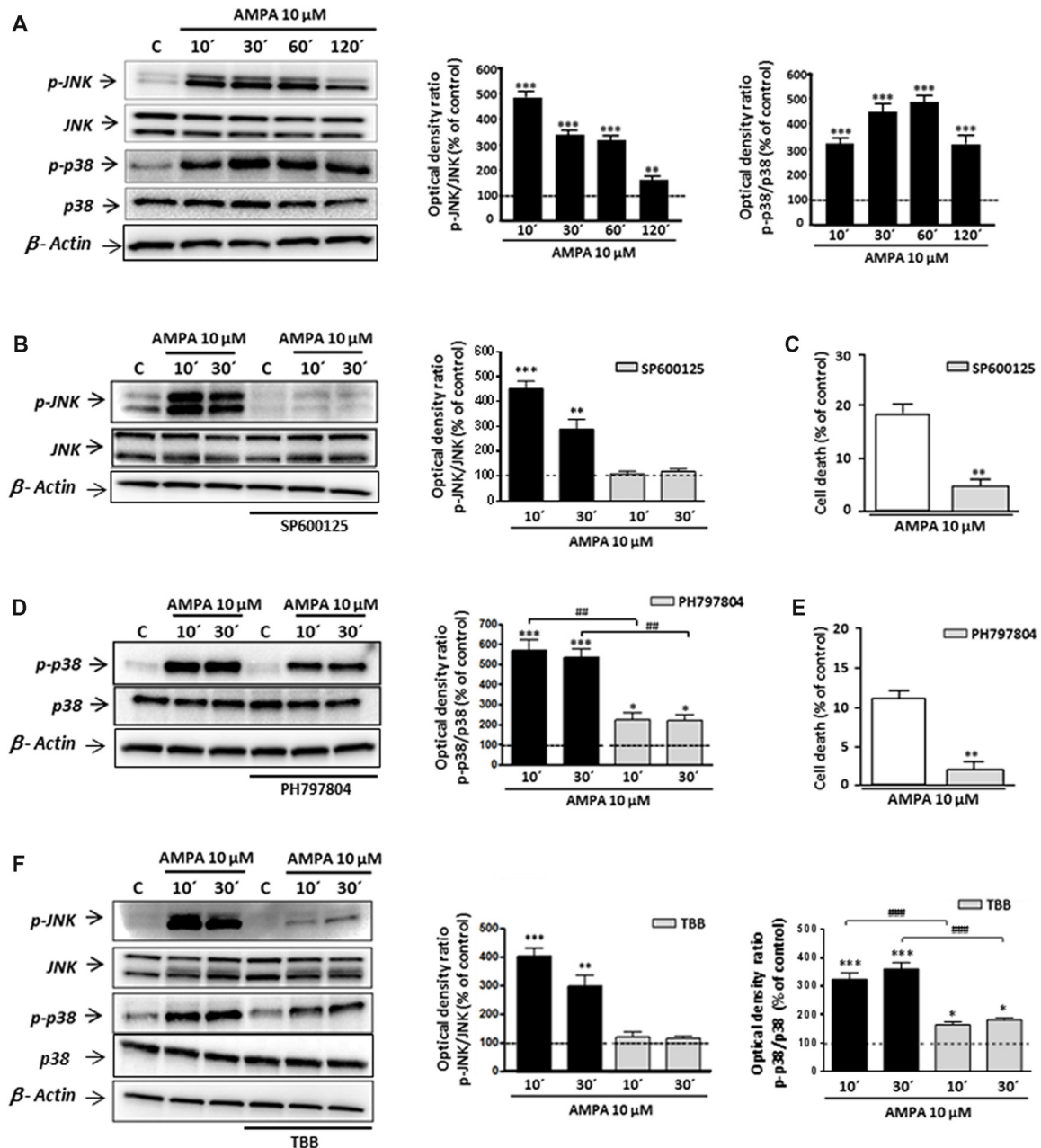


FIGURE 3 | AMPA-induced c-Jun N-terminal kinase (JNK)/p38 apoptotic activation depends on CK2 activity. Oligodendrocytes were treated with 10 μM AMPA for 30 min, in the presence of 100 μM CTZ, and total lysates were harvested at the indicated times. When indicated, the stimulus was performed in the presence of the corresponding inhibitor. **(A)** Activation of AMPA receptors triggered an early and potent increase in the JNK and p38 phosphorylation levels at 10, 30, 60 and 120 min after AMPA treatment, determined by WB analysis. **(B,D)** The early AMPA-induced activation of JNK and p38 was prevented by the presence of 1 μM inhibitor SP600125 or PH797804, respectively. **(C,E)** The inhibition of JNK or p38 by SP600125 or PH797804, significantly reduced cell death induced by AMPA receptor activation in oligodendrocytes. **(F)** Intense JNK and p38 phosphorylation induced by exposure to AMPA was significantly reduced in the presence of CK2 inhibitor (TBB; 5 μM) at both times analyzed (10 and 30 min post-stimuli). **p* < 0.05, ***p* < 0.01, ****p* < 0.001 (cells treated with AMPA vs. control cells); ##*p* < 0.01, ###*p* < 0.001 (cells treated with each mitogen-activated protein kinases (MAPKs) inhibitor vs. cells treated with only AMPA).

PLP-DsRed⁺ oligodendrocytes in these preparations and we observed that AMPA treatment also reduced by almost half the cellular number compared with control (140.5 ± 13.9 vs. 266.2 ± 13.9 per FOV, respectively; **Figure 4F**). As in the

previous analysis, the inhibition of CK2 or JNK during the AMPA receptor activation completely avoided the effect caused by agonist (227.5 ± 13.6 cells for TBB and 252.5 ± 18.9 cells for SP600125).

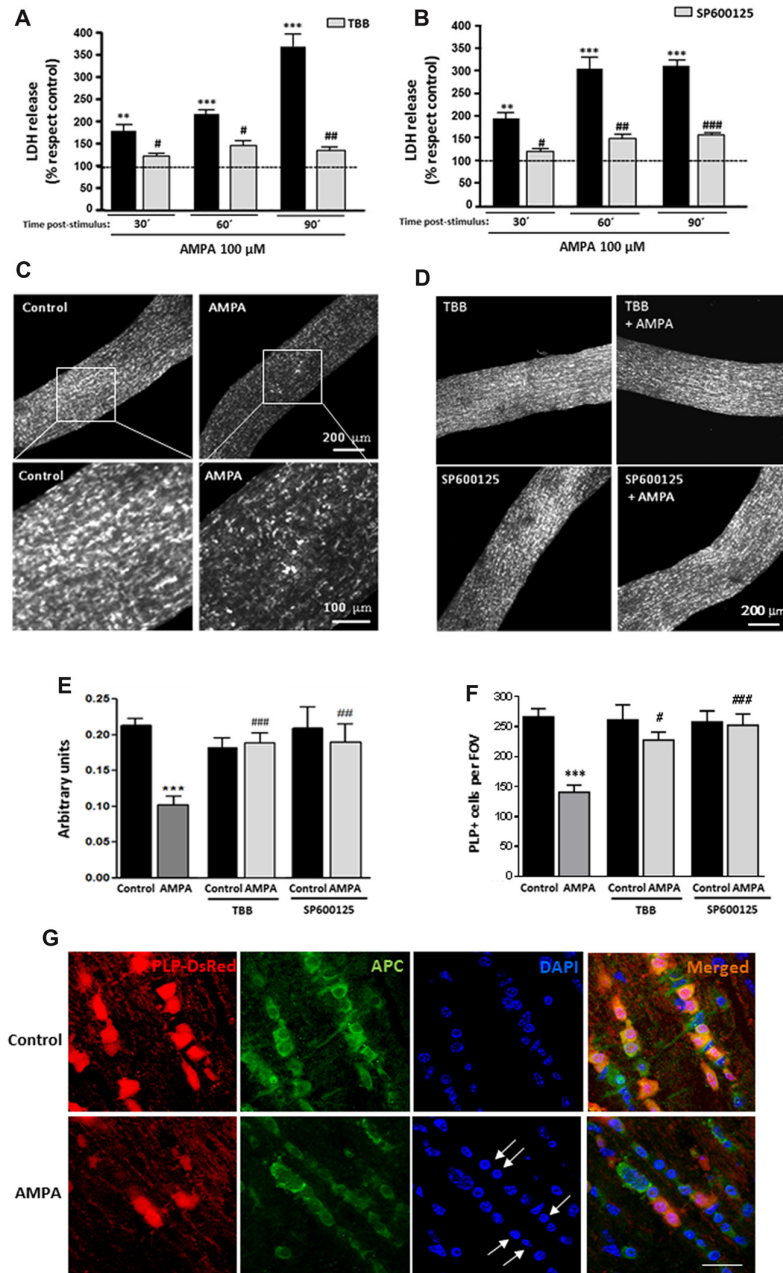


FIGURE 4 | AMPA provokes oligodendroglial damage in isolated optic nerves from PLP-DsRed transgenic mice. Isolated optic nerves from PLP-DsRed transgenic mice were preincubated in artificial CSF medium in absence or presence of TBB (25 μ M; 3 h) or SP600125 (20 μ M; 1 h) and subjected to excitotoxic insult by stimulation of AMPA receptors (100 μ M CTZ plus 100 μ M AMPA) during 2 h. **(A,B)** Lactate dehydrogenase (LDH) release quantification at 30, 60 and 90 min post-stimulus showed that TBB or SP600125 pre-treated optic nerves exhibited a significant reduction in LDH release at all post-stimulus times analyzed. $**p < 0.005$; $***p < 0.0001$ (optic nerves treated with AMPA vs optic nerves control); $#p < 0.05$; $##p < 0.01$; $###p < 0.001$ (vs. optic nerves treated only with AMPA). **(C,D)** Representative fields of z-stacks of optic nerves from PLP-DsRed transgenic mice control or stimulated with AMPA alone **(C)** or in presence of inhibitors TBB or SP600125 **(D)**. Note a loss of oligodendrocytes in optic nerves exposed to AMPA, which was prevented by incubation of agonist in presence of TBB or SP600125. **(E)** Quantification of the fluorescence signal emitted by oligodendrocytes of optic nerves from P25 PLP-DsRed mice, expressed as arbitrary units of fluorescence. $***p < 0.001$ (optic nerves treated with AMPA vs. optic nerves control); $##p < 0.01$, $###p < 0.001$ (vs. optic nerves treated only with AMPA). **(F)** Cell counts of PLP+ oligodendrocytes were performed and data were represented as mean number of cells (\pm SEM, $n > 4$ animals) in a constant volume (FOV), as detailed in “Materials and Methods” section. $***p < 0.001$ (optic nerves treated with AMPA vs. optic nerves control); $#p < 0.05$, $###p < 0.001$ (vs. optic nerves treated only with AMPA). Both quantifications show that oligodendrocyte loss induced by AMPA excitotoxic insult was inhibited by the presence of TBB or SP600125 inhibitors. **(G)** Optic nerves from PLP-DsRed transgenic mice were processed for immunofluorescence using antibodies to APC and nuclei were stained with DAPI. Treatment with AMPA induced a dramatic fluorescence loss in both PLP and APC oligodendroglial markers, indicating severe oligodendrocyte damage. In addition, DAPI labeling revealed nuclei condensation in AMPA-treated optic nerves (arrows). Scale bar 20 μ m.

Finally and to corroborate the effect of AMPA exposure in viability of oligodendrocytes we assayed the status of the oligodendrocyte marker APC (Ab-7) and their nuclei by DAPI staining, in cryosections of optic nerves from control and AMPA-treated PLP-DsRed mice (**Figure 4G**). Then, immunohistochemistry of optic nerves confirmed that oligodendrocytes were severely damaged by AMPA as they showed loss of PLP-DsRed, as it had previously been described, and reduction in the APC expression and these alterations were accompanied with chromatin condensation revealed by DAPI staining (arrows in **Figure 4G**).

These results in whole optic nerves *ex vivo* further assessed the observations described above showing that activation of AMPA receptors triggered apoptotic cell death in oligodendrocytes and the tandem CK2-JNK plays a key role in execution of this apoptotic program. These data, in combination with results obtained from *in vitro* kinase assay, suggests that a greater degree of vulnerability of oligodendrocytes to AMPA may be linked to a higher degree of activation of CK2 kinase, which in turn, mediates subsequent JNK activation that culminates in cell death.

Gene Silencing of CK2 Reduced AMPA-Induced Oligodendrocyte Cell Death and Associated JNK Activation

To confirm the contribution of CK2-JNK to excitotoxic cascade initiated by AMPA in oligodendrocytes, we next knocked down endogenous CK2 expression in these cells by transfecting CK2 shRNA. First, we observed that CK2 shRNA (sh-CK2) but not control shRNA (sh-Scrambled) significantly reduced the endogenous level of CK2 up to $73.28 \pm 2.65\%$ (**Figure 5A**). Next, oligodendrocytes from each of these experimental conditions were subjected to AMPA treatment and then we quantified the toxicity level caused by the agonist in these cells (**Figure 5B**). Consistent with the cytoprotective effect achieved by CK2 pharmacological inhibitors (TBB, DRB or resofurin), we observed that AMPA-triggered oligodendrocyte death was significantly reduced in cells transfected with sh-CK2, compared with sh-Scrambled transfected cells ($2.3 \pm 1.8\%$ vs. $16.6 \pm 2.8\%$, respectively). These results confirm that CK2 is involved in the harmful process initiated by AMPA in oligodendrocytes.

Because CK2 and JNK operate together in triggering cell death events, and based on our results described above, we tried to determine if knocking down of endogenous CK2 affects JNK phosphorylation after AMPA exposure. As showed in **Figure 5C**, we observed significant increase of JNK phosphorylation level in Sh-Scrambled transfected cells after AMPA receptors stimulation ($173.6 \pm 15.8\%$, respect to untreated cells, 100%). However, knocking down CK2 oligodendrocytes subjected to the same AMPA stimulus showed no increment in JNK phosphorylation degree, with values close to the control ($92.4 \pm 3.8\%$ respect to 100% control). It should be noted that in these knocking down cells could be verified a remarkable decrease in the expression of CK2, both in control cells and treated with AMPA (**Figure 5C**).

Overall, these observations are consistent with pharmacological CK2 inhibition and further assess that CK2 plays a key role in AMPA-induced oligodendroglial toxicity by interfering with JNK pro-apoptotic activation.

p53 Is a Downstream Pro-apoptotic Effector of CK2/JNK Signaling Cascade in AMPA-Induced Oligodendrocyte Cell Death

One potential target of pro-apoptotic signaling by JNK is the tumor suppressor p53 (Dhanasekaran and Reddy, 2008; Choi et al., 2011; Saha et al., 2012). Additionally, the involvement of CK2 kinase in the p53 phosphorylation process is essential for activation of p53 and its entry into cell pro-death programs and apoptosis (Sayed et al., 2001; Meek and Cox, 2011; Rao et al., 2014). Moreover, p53 participates in neuronal glutamatergic excitotoxicity (Choi et al., 2011; Shah et al., 2014), so we explored the role of p53 in oligodendroglial excitotoxicity and its potential interaction with CK2-JNK.

Initially, we analyzed the status of p53 in oligodendrocytes and, as shown in **Figure 6A**, we detected an increase in the levels of total p53 in oligodendrocytes following the stimulation of AMPA receptors ($10 \mu\text{M}$, 30 min), analyzed at 30 min after the withdrawal of the agonist. This change can indicate an increase in the stability of p53, which can be associated with its role as transcription factor (Allende-Vega et al., 2013; Loughery and Meek, 2013) and its consequent participation in apoptosis.

To analyze the possible transcriptional activity of p53 in oligodendrocyte excitotoxicity, we determined by qPCR the gene expression of molecules interacting with the p53 system, as MDM2 and PUMA. As shown in **Figure 6B**, activation of AMPA receptors in oligodendrocytes caused a rapid and sustained increase in mRNA levels of MDM2, which was statistically significant at 30 min after application of the agonist. On the other hand, activation of receptors in oligodendrocytes caused a significant increase in PUMA levels (**Figure 6B**), a small protein of Bcl-2 family that is induced by transcriptional activation of p53 and acts as a key mediator of cytosolic proapoptotic p53 function. These data are in agreement with those documented by other authors in p53-dependent apoptotic contexts (Yu et al., 2003; Antony et al., 2012).

Based on these results, we examined the contribution of p53 on excitotoxic damage by evaluating AMPA-induced cell death in presence of p53 inhibitors, pifithrin- α and pifithrin- μ . Pre-treated oligodendrocytes with $20 \mu\text{M}$ pifithrin- α or $1 \mu\text{M}$ pifithrin- μ were less vulnerable to AMPA exposure, so the cell death was of $9.8 \pm 1.2\%$ or $11.0 \pm 1.8\%$, respectively, compared to $20.7 \pm 2.1\%$ observed in cells treated only with agonist (**Figure 6C**). Furthermore, p53 inhibition also reduced AMPA-triggered mitochondrial dysfunction analyzed by ROS production and loss of mitochondrial transmembrane potential (**Figures 6D,E**). Thus, we observed ROS levels significantly increased after activation of AMPA receptors (up to $164.2 \pm 20.8\%$), an effect that was abolished in the presence of pifithrin- α or pifithrin- μ ($77.2 \pm 14.5\%$ or $100.4 \pm 7.8\%$, respectively; **Figure 6D**). Besides, JC-1 probe fluorescence

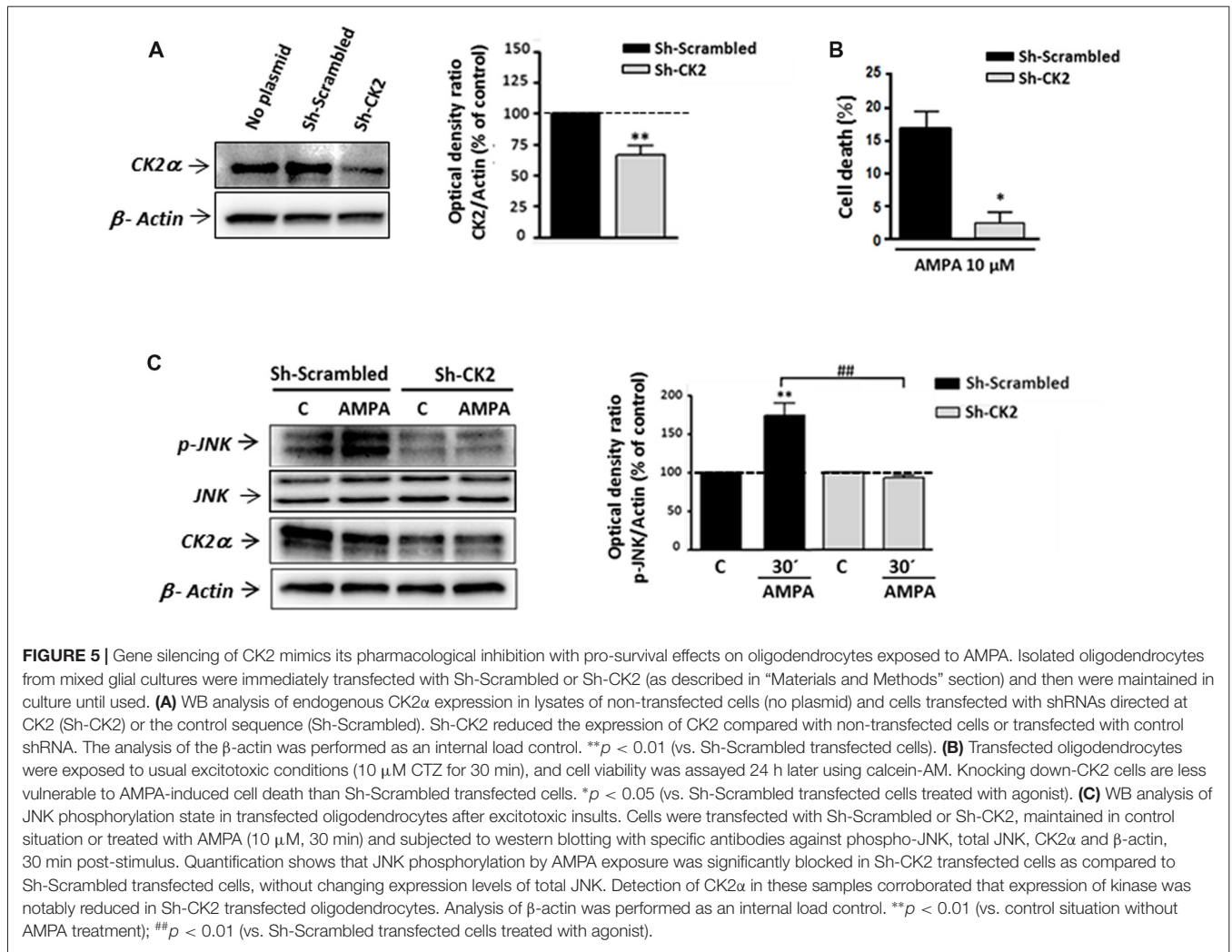


FIGURE 5 | Gene silencing of CK2 mimics its pharmacological inhibition with pro-survival effects on oligodendrocytes exposed to AMPA. Isolated oligodendrocytes from mixed glial cultures were immediately transfected with Sh-Scrambled or Sh-CK2 (as described in “Materials and Methods” section) and then were maintained in culture until used. **(A)** WB analysis of endogenous CK2 α expression in lysates of non-transfected cells (no plasmid) and cells transfected with shRNAs directed at CK2 (Sh-CK2) or the control sequence (Sh-Scrambled). Sh-CK2 reduced the expression of CK2 compared with non-transfected cells or transfected with control shRNA. The analysis of the β -actin was performed as an internal load control. ** $p < 0.01$ (vs. Sh-Scrambled transfected cells). **(B)** Transfected oligodendrocytes were exposed to usual excitotoxic conditions (10 μ M CTZ for 30 min), and cell viability was assayed 24 h later using calcein-AM. Knocking down-CK2 cells are less vulnerable to AMPA-induced cell death than Sh-Scrambled transfected cells. * $p < 0.05$ (vs. Sh-Scrambled transfected cells treated with agonist). **(C)** WB analysis of JNK phosphorylation state in transfected oligodendrocytes after excitotoxic insults. Cells were transfected with Sh-Scrambled or Sh-CK2, maintained in control situation or treated with AMPA (10 μ M, 30 min) and subjected to western blotting with specific antibodies against phospho-JNK, total JNK, CK2 α and β -actin, 30 min post-stimulus. Quantification shows that JNK phosphorylation by AMPA exposure was significantly blocked in Sh-CK2 transfected cells as compared to Sh-Scrambled transfected cells, without changing expression levels of total JNK. Detection of CK2 α in these samples corroborated that expression of kinase was notably reduced in Sh-CK2 transfected oligodendrocytes. Analysis of β -actin was performed as an internal load control. ** $p < 0.01$ (vs. control situation without AMPA treatment); ## $p < 0.01$ (vs. Sh-Scrambled transfected cells treated with agonist).

quantification at different times post-stimulus showed that AMPA receptor activation induced a loss of mitochondrial potential post-stimulation reaching minimum levels between 30 and 60 min ($58.6 \pm 5.6\%$; $59.2 \pm 9.3\%$, respectively). In contrast, the mitochondrial potential in p53 inhibitor pre-treated oligodendrocytes showed a significant recovery, with values near to control after 90 min post-stimulus (**Figure 6E**).

Finally, we analyzed by WB the effect of pifithrin on total p53 and PUMA protein expression following the excitotoxic insult (**Figure 6F**). AMPA treatment provoked significant increases in p53 and PUMA protein level ($180.3 \pm 11.5\%$ and $159.7 \pm 13.5\%$, respect to 100% control), observed at 30 min post-stimulus, which were attenuated by pifithrin in both cases ($111.5 \pm 4.4\%$ for p53 and $124.7 \pm 14.2\%$ for PUMA).

Once the participation of p53 in the excitotoxic process was established, we analyzed the possible linkage between p53, CK2 and JNK based on that CK2 can directly phosphorylate p53 and modulate its transcriptional activity (Sayed et al., 2001; Keller and Lu, 2002), or indirectly through the CK2-initiated pathway and executed by JNK. To study the possibilities we first

performed co-immunoprecipitation assays between CK2-p53 in which we immunoprecipitated the CK2 α protein in control oligodendrocytes and treated with 10 μ M AMPA for 30 min and recollected at 10, 30 and 60 min later. Then, we detected by WB the presence of p53 in the immunoprecipitated samples (**Figure 7A**).

The results showed that the amount of p53 linked to CK2 α rapidly increased after AMPA treatment, indicating a fast, powerful and direct molecular interaction between CK2 α and p53. However, this union decreased over time so that at 10 min after AMPA elimination the binding p53-CK2 α reached a level of $210.0 \pm 19.1\%$, at 30 min was of $179.0 \pm 20.2\%$, and at 60 min was of $137.1 \pm 23.9\%$, compared with 100% of control (**Figure 7B**).

In addition, by immunofluorescence staining we observed that AMPA early induced both p53 activation and its nuclear localization and these events were significantly reduced in oligodendrocytes pre-treated with CK2 inhibitor TBB (5 μ M; pretreatment 3 h; **Figure 7C**). To quantify this effect, we counted the oligodendrocytes that showed p53 in the nucleus (stained with DAPI) in cultures exposed to different situations and we

could be observed that AMPA caused a significant increase in nuclear location of p53 after 30 min (37.3 ± 1.6 cells per field) and 60 min (17.8 ± 3.6), compared to control cells ($5, 4 \pm 0.9$ cells per field). However, the presence of TBB significantly reduced the number of oligodendrocytes showing nuclear p53 after AMPA exposure and analyzed 30 min later (8.8 ± 1.9 cells per field; **Figure 7D**). Together, these data suggest that CK2 participates, at least in part, in p53 activation in oligodendrocytes subjected to the stimulation of AMPA receptors.

Ser15 Phosphorylation of p53 Following AMPA Exposure Is JNK and CK2 Dependent

Apoptotic stimuli can lead to rapid and substantial multisite phosphorylation of p53 by different kinases, nucleated initially through phosphorylation of Serine 15 (Jones et al., 2005; Meek, 2009). This suggests a key and possibly universal role in promoting p53-transcription function (Loughery et al., 2014). In addition, this post-transcriptional modification of p53 has been related with its mitochondrial insertion and pro-apoptotic interaction with proteins of Bcl-2 family (Park et al., 2005; Nieminen et al., 2013; Wang et al., 2015).

With the aim of investigating this possibility in our experimental paradigm, we carried out immunoprecipitation assays to detect the presence of p53 phosphorylated in the residue Serine15, p-p53 (Ser15), in control oligodendrocytes and subjected to excitotoxic damage (10 μ M AMPA in presence of 100 μ M CTZ for 30 min). For that, total p53 protein was immunoprecipitated by binding agarose beads to an anti-total p53 antibody, applying the protocol described in "Materials and Methods" section (IP: p53; **Figure 8A**). Then, the immunoprecipitates were subjected to WB using a specific antibody (anti-p-p53 (Ser15)) to detect the presence of the Ser15 phosphorylated p53 fraction both in control and treated oligodendrocytes. This specific antibody detects endogenous levels of p53 only when phosphorylated at Ser15 and does not cross-react with p53 phosphorylated at other sites.

As shown in **Figure 8A**, there was an increase in p53 phosphorylation at Ser15 induced by AMPA, especially remarkable at 30 and 60 min after withdrawal of the AMPA stimulus. In addition, the presence of p-p53 (Ser15) was also determined by immunocytochemistry in oligodendrocytes control and stimulated with 10 μ M AMPA for 30 min (**Figure 8B**). The treatment induced a notable increase in the presence of p-p53 (Ser15) and, importantly, this phosphorylated p53 was predominantly located in cell regions stained with COX-IV antibody, suggesting a mitochondrial redistribution triggered by AMPA receptor activation. In addition, although some studies have also described the presence of p-p53 (Ser15) at the nuclear level (Li et al., 2010; Jin et al., 2013), we have seen total absence of this residue in the nucleus of oligodendrocytes after AMPA receptor stimulation (**Figure 8C**).

Finally, and based on the literature describing that JNK and p53 may also directly interact (Saha et al., 2012; Shi et al., 2014), we next analyzed the behavior of

p53 and p-p53 (Ser15) in oligodendrocytes stimulated with AMPA in absence or presence of JNK inhibitor SP600125.

As shown in **Figure 9A**, WB analysis of p53 levels after AMPA receptor stimulation (AMPA 10 μ M plus CTZ 100 μ M, 30 min), showed that excitotoxic insults increased p53 expression at 30 and 60 min after stimulus ($260.7 \pm 22.5\%$ and $273.3 \pm 26.0\%$, respectively and compared to control cells). The presence of JNK inhibitor SP600125 1 μ M significantly reduced that effect ($166.7 \pm 14.5\%$ y $169.3 \pm 17.8\%$, respectively, compared to control cells). In addition, we detected a robust AMPA-triggered phosphorylation of p53 at Ser15 after 30 min ($350.7 \pm 27.3\%$) and 60 min ($256 \pm 30.1\%$) that was not observed in presence of JNK inhibitor ($118.2 \pm 10.8\%$ and $115.6 \pm 16.7\%$, respectively).

These results were also corroborated by immunocytochemistry. Oligodendrocytes were treated with AMPA plus CTZ, in the absence or presence of 1 μ M SP600125 (**Figures 9B,C**). Changes in the total expression of p53, associated with its activation, were determined using the p53 antibody recognizing total p53 and the presence of phosphorylation in Ser15 was detected by the specific antibody p-p53 (Ser15). As shown in **Figure 9B**, cells treated with AMPA displayed p53 activation (green) which was not observed in control and AMPA plus SP600125-treated cells. Additionally, JNK inhibition prevented AMPA-induced phosphorylation of p53 at Ser15 and therefore, its location in the cellular areas stained with the COX-IV antibody was diminished (**Figure 9C**).

On the other hand, our co-immunoprecipitation experiments support a direct interaction between CK2 and p53. For that, and in order to check the possible role of CK2 in the phosphorylation of p53 at Ser15 and its translocation into mitochondria, we activated AMPA receptors in oligodendrocytes in presence of CK2 inhibitor TBB and analyzed by immunocytochemistry the expression of p53 (**Figure 9B**) and p-p53 (Ser15; **Figure 9C**). The results indicated that CK2 inhibition reduced both total p53 and p-p53 (Ser15) expression triggered by AMPA, as well as its mitochondrial accumulation.

These results suggest a sequential activation of the CK2/JNK/p53 axis triggered by the overstimulation of AMPA receptors in oligodendrocytes, which will lead to cell death by apoptosis.

DISCUSSION

As oligodendrocytes are highly vulnerable to overactivation of GluRs, oligodendroglial excitotoxicity may be considered a major factor in demyelinating disorders of the CNS like MS disease. Under pathologic conditions, several components of the glutamate system are altered, compromising glutamate homeostasis. Proinflammatory cytokines (e.g., TNF α and IL-1 β) negatively regulate glutamate transporter expression and activity of, raising extracellular glutamate concentrations (Tilleux and Hermans, 2007). In turn, immune activation increases cystine-glutamate exchanger (xCT) expression that may result in higher glutamate release and excitotoxic damage to oligodendrocytes (Domercq et al., 2007; Pampliega et al., 2011).

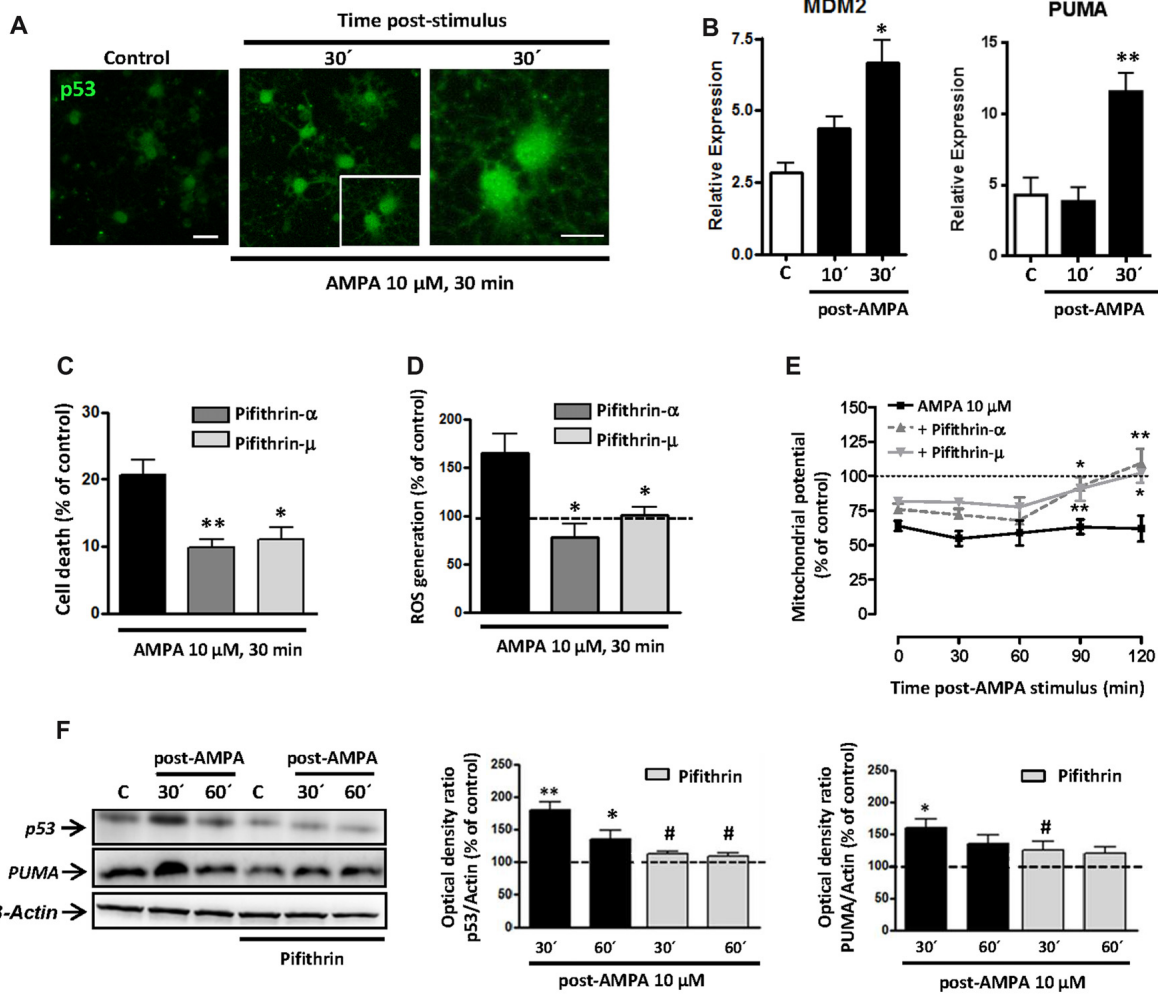
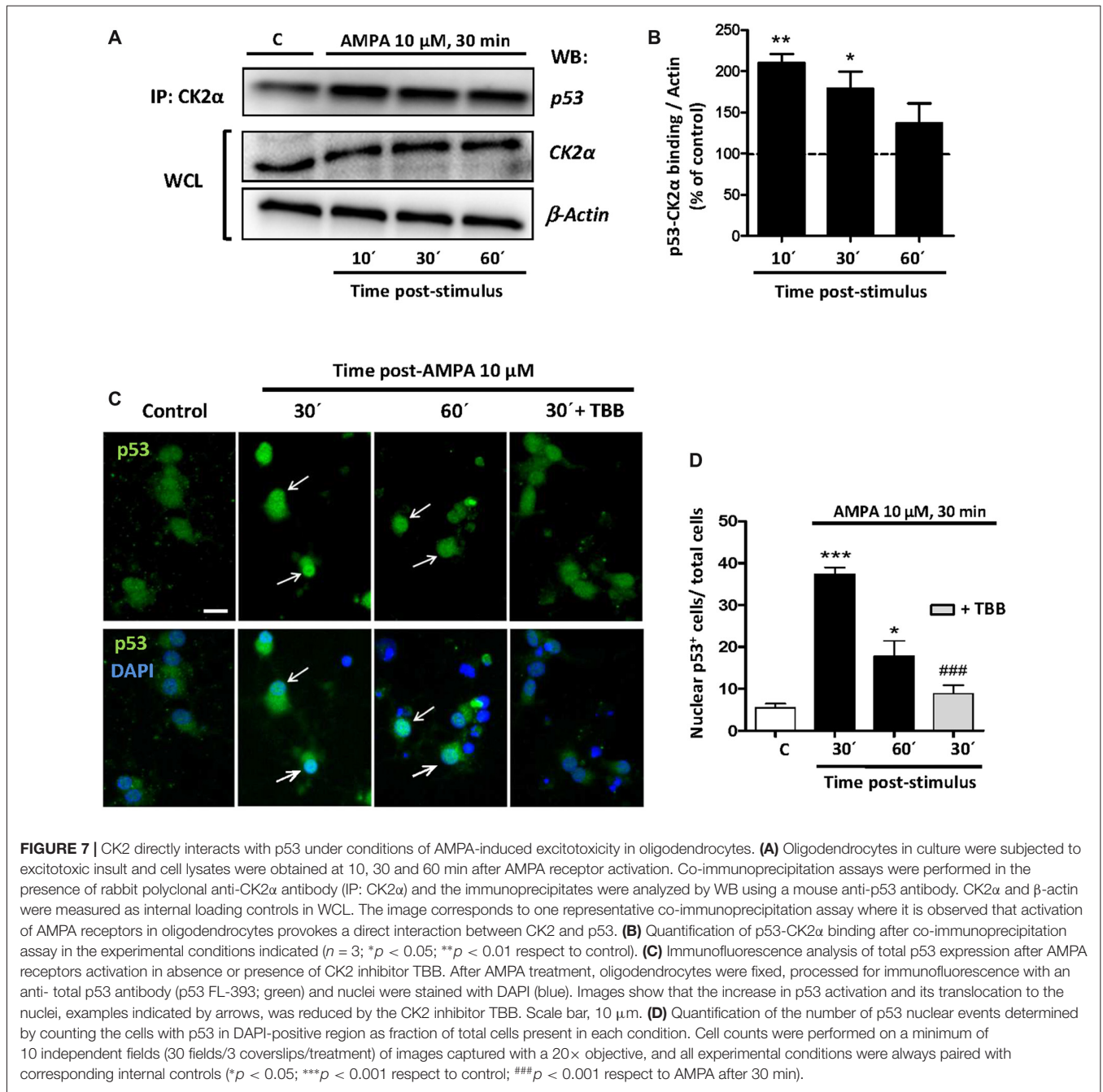


FIGURE 6 | AMPA excitotoxic insult induces p53 stabilization and transcriptional activation in oligodendrocytes, which is inhibited by pifithrin. Oligodendrocytes were exposed to 10 μM AMPA together with 100 μM CTZ for 30 min. **(A)** Immunofluorescence analysis of p53 expression. After AMPA receptor activation, at 30 min post-stimulus, cells were processed for p53 immunofluorescence using the p53 (FL-393) antibody, which recognized total p53. Exposure to AMPA triggered a notable increase in the expression of total p53 (green). Scale bar, 20 μm (left and central images); 10 μm (right image). **(B)** RT-PCR analysis for expression of p53 transcriptional targets, MDM2 and PUMA, showed a significant rise in their relative expression in cultured oligodendrocytes after AMPA receptor activation. ($n \geq 3$; $*p < 0.05$, $**p < 0.01$ respect to untreated control cells). **(C)** AMPA-induced excitotoxicity was significantly reduced in the presence of p53 inhibitors, pifithrin-β (20 μM) or pifithrin-μ (1 μM), preincubated for 1 h before the activation of AMPA receptors. ($*p < 0.05$, $**p < 0.01$, respect to cells treated only with AMPA). **(D)** ROS generation triggered by activation of AMPA receptors was attenuated by p53 inhibitors. Oligodendrocytes were exposed to 10 μM AMPA for 30 min in absence or presence of pifithrin and ROS level was immediately determined using the dye CM-DCFDA (10 μM, Molecular Probes) and measuring the signal in a Synergy-HT fluorimeter. Results showed that levels of ROS induced by AMPA were attenuated in oligodendrocytes pretreated with both pifithrin-α or pifithrin-μ. Data represent mean \pm SEM ($n = 3$; $*p < 0.05$, compared with cells treated only with agonist). **(E)** In addition, mitochondrial membrane potential was quantified by fluorimetry at different times after AMPA stimulus, by loading cells with dye JC-1 (3 μM, Molecular Probes). Mitochondrial depolarization induced by excitotoxic insult was attenuated in pifithrin-α and pifithrin-μ pre-treated oligodendrocytes, as compared with cells treated only with agonist. Data are represented as mean \pm SEM compared with cells treated only with AMPA for each time point analyzed ($n \geq 3$; $*p < 0.05$; $**p < 0.01$). **(F)** Oligodendrocytes were preincubated with pifithrin-μ (1 μM) before AMPA receptor activation and total protein was collected 30 and 60 min later for WB analysis. The presence of p53 inhibitor pifithrin-μ during excitotoxic signals reduced p53 and PUMA accumulation induced by AMPA. The analysis of β-actin was performed as an internal load control and was used to quantify the expression level of p53 and PUMA in each condition. ($*p < 0.05$, $**p < 0.01$ respect to control cells; # $p < 0.05$ respect to cells treated only with AMPA).

Together, these and other alterations cause an increase in extracellular levels of glutamate that mediates the overactivation of Ca²⁺-permeable GluRs in oligodendrocytes and contributes to tissue damage in demyelinating diseases and other oligodendropathies. Indeed, AMPA and kainate receptor antagonists ameliorate neurological symptoms in several forms

of EAE used to model various stages of MS (Bolton and Paul, 2006; Matute et al., 2001; Matute, 2011).

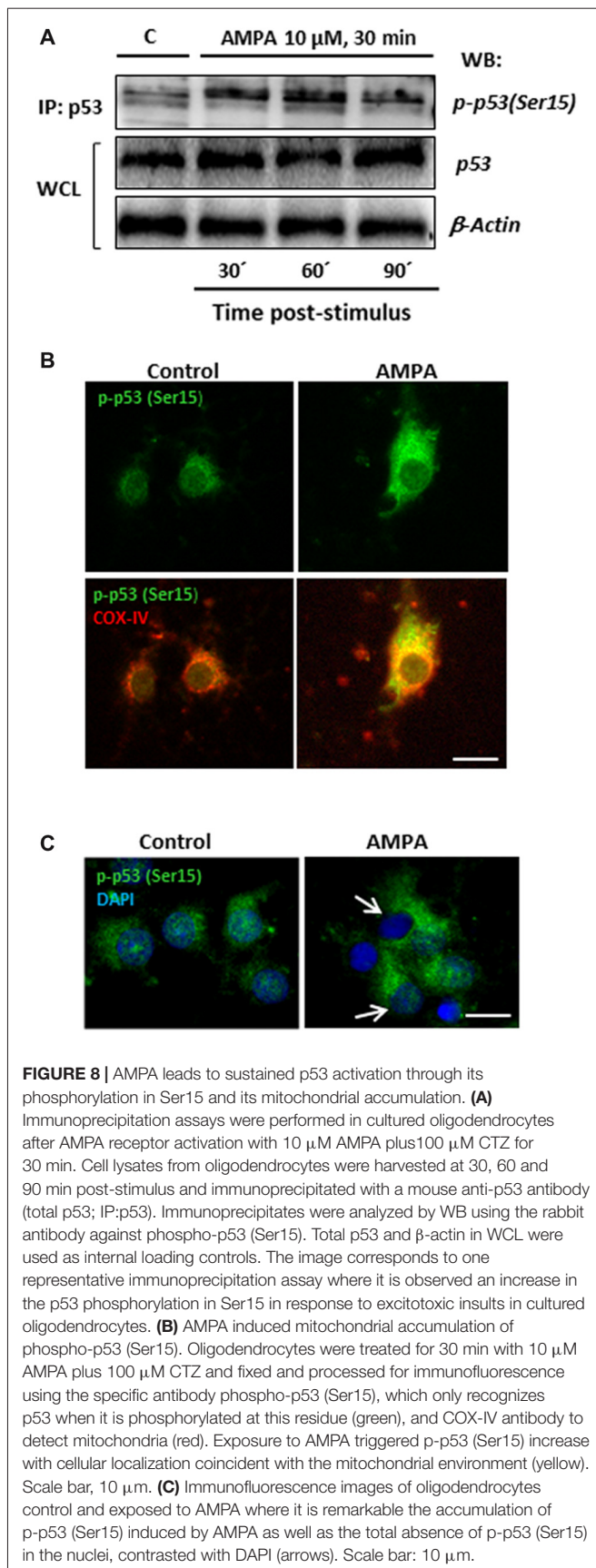
The apoptotic program activated by AMPA receptor-mediated excitotoxic insults in oligodendrocytes has not been fully elucidated, and knowing it in detail could provide the necessary tools to develop effective protective therapies.



The results reported here show that apoptosis induced by excitotoxicity in oligodendrocytes is mediated by a JNK and p38 signaling cascade in a CK2-dependent manner. In addition, we found that p53 is activated in response to excitotoxic insults initiated by AMPA receptors, and that this activation is a downstream consequence of, at least, CK2 and JNK proapoptotic contribution. These data provide novel targets to limit oligodendroglial cell death triggered by glutamate excitotoxicity.

On the basis that CK2 is generally part of main prosurvival signaling pathways (Turowec et al., 2010; Zheng et al., 2011;

Gray et al., 2014) our initial hypothesis was that CK2 could limit deleterious consequences of AMPA receptor activation in oligodendrocytes. Unexpectedly, AMPA excitotoxic insults trigger an increase in CK2 activity and both pharmacological inhibition and CK2 gene silencing attenuates toxicity induced by AMPA receptors stimulation in oligodendrocytes, concomitant with the interruption of the cascade of events leading to mitochondrial dysfunction. Thus, CK2 inhibition in oligodendrocytes attenuated depolarization of the mitochondrial membrane, which is an early event in apoptosis (for review see Atlante et al., 2001; Skulachev, 2006), as well as it reduced



oxidative stress. These observations indicate that CK2 is required as part of the early apoptotic machinery that distort mitochondrial function in response to excitotoxic insults to oligodendrocytes, and suggest a proapoptotic role for CK2 in the regulation of oligodendrocyte cell death. Consistent with our results, renal ischemia/reperfusion injury results in increased CK2 α expression, and CK2 inhibition attenuated inflammation and oxidative stress which results in reduced apoptosis and concomitant renal dysfunction (Ka et al., 2015). Conversely, reduced CK2 expression levels and lower total activity of this kinase, after mice cerebral ischemic injury, facilitates ROS production and mediates neuronal cell death (Kim et al., 2009).

Our findings indicate that CK2 regulates a central proapoptotic signaling pathway activated upon AMPA receptor stimulation. Along this line, CK2 can have a pro-apoptotic role in cellular events that involve JNK activation and CK2-JNK interactions (Min et al., 2003; Hilgard et al., 2004). JNK are important stress-responsive kinases that are activated by various forms of insults, including ischemia (Nijboer et al., 2011) and glutamate excitotoxicity (Shah et al., 2014). Additionally, JNK signaling is involved in neuroinflammation, blood barrier disruption and oligodendroglial apoptosis in white matter injury (Wang et al., 2012). In the current study, we observed that JNK signaling pathway activated by AMPA receptor stimulation involves the joint activation of p38 pathway. This phenomenon presumably occurs via ASK1, a MAPK kinase that activates downstream MAPKs, JNK and p38, and regulates neuroinflammation and demyelination by TLR-ASK1-p38 pathway (Guo et al., 2010). In line with this idea, we have recently observed that ASK1 pharmacological inhibition with NQDI reduces AMPA-induced oligodendrocyte cell death and that this protection is based on the ability to inhibit downstream JNK and p38 activation (data not shown).

In the current study, we have also found a link between the activation of CK2, JNK and p38. Thus, CK2 pharmacological inhibition with TBB jointly reduces JNK and p38 activation after AMPA excitotoxic insult. This suggests that CK2 acts as a link between early stress events induced by AMPA excitotoxicity in oligodendrocytes and pro-apoptotic activation of hypothetical JNK/p38 axis.

The tumor suppressor transcription factor p53 plays a central role in induction of cell-cycle arrest, senescence, and apoptosis in the response to a variety of prolonged or severe stresses (Loughery and Meek, 2013) and a number of p53-modifying enzymes have been identified, for example MAPK p38 and JNK (Wu, 2004; Cargnello and Roux, 2012). The link between JNK/p38 activation and p53 apoptotic contribution has also been previously described in glutamatergic excitotoxicity conditions in hippocampal neurons and differentiated PC12 cells (Choi et al., 2011; Jiang et al., 2014). Thus, knock-down or blockade of JNK inhibited glutamate-induced p53 activation in that excitotoxic paradigm (Choi et al., 2011). In the present study, we observed that p53 may be one of the downstream consequences of CK2/JNK signaling pathway activation, since both CK2 or JNK inhibition were able to limit p53 activation/stabilization

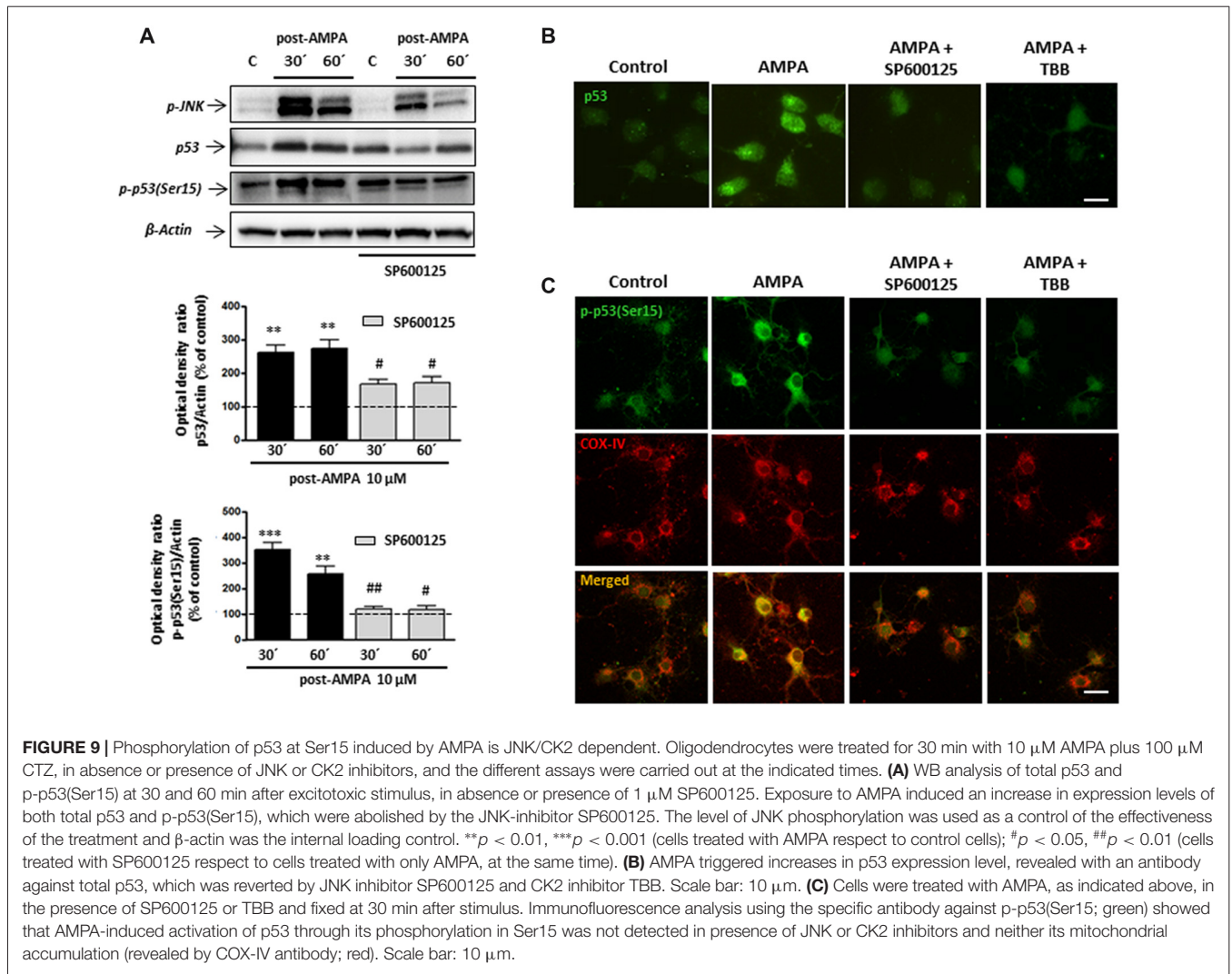


FIGURE 9 | Phosphorylation of p53 at Ser15 induced by AMPA is JNK/CK2 dependent. Oligodendrocytes were treated for 30 min with 10 μ M AMPA plus 100 μ M CTZ, in absence or presence of JNK or CK2 inhibitors, and the different assays were carried out at the indicated times. **(A)** WB analysis of total p53 and p-p53(Ser15) at 30 and 60 min after excitotoxic stimulus, in absence or presence of 1 μ M SP600125. Exposure to AMPA induced an increase in expression levels of both total p53 and p-p53(Ser15), which were abolished by the JNK-inhibitor SP600125. The level of JNK phosphorylation was used as a control of the effectiveness of the treatment and β -actin was the internal loading control. ** $p < 0.01$, *** $p < 0.001$ (cells treated with AMPA respect to control cells); # $p < 0.05$, ## $p < 0.01$ (cells treated with SP600125 respect to cells treated with only AMPA, at the same time). **(B)** AMPA triggered increases in p53 expression level, revealed with an antibody against total p53, which was reverted by JNK inhibitor SP600125 and CK2 inhibitor TBB. Scale bar: 10 μ m. **(C)** Cells were treated with AMPA, as indicated above, in the presence of SP600125 or TBB and fixed at 30 min after stimulus. Immunofluorescence analysis using the specific antibody against p-p53(Ser15; green) showed that AMPA-induced activation of p53 through its phosphorylation in Ser15 was not detected in presence of JNK or CK2 inhibitors and neither its mitochondrial accumulation (revealed by COX-IV antibody; red). Scale bar: 10 μ m.

status induced by AMPA excitotoxic insult. This suggests that in oligodendrocyte excitotoxicity CK2 mediates p53 activation through JNK phosphorylation. Ser15 phosphorylation is required for p53 function in the physiological context of p53-responsive promoters that suggests a key role even for low levels of this modification in promoting p53-transcription function (Loughery et al., 2014). Accordance with this, we propose the modulation of p53 phosphorylation at the Ser15 through CK2/JNK as an essential step in oligodendrocyte apoptotic death, alone or in conjunction with p38, as described in previous reports (Gong et al., 2010; Fausti et al., 2013).

So, the fact that both CK2 and JNK inhibition mediated reduction in mitochondrial phospho-p53 (Ser15) could be indicating that these kinases are the mediators of a mitochondrial specific p53 modification implicated in AMPA-induced oligodendrocyte cell death.

On the other hand, our co-immunoprecipitation experiments support a direct interaction between CK2 and p53. In this sense, CK2 in a complex with the chromatin factor FACT

(hSPT16 and SSRP1), was identified as the kinase responsible for p53 phosphorylation at Ser392 after UV exposure *in vitro* (Keller et al., 2001; Finlan et al., 2006). Thus, CK2 catalytic activity towards p53 is enhanced by FACT *in vitro*, and Ser392 phosphorylation leads to an increase in p53 DNA binding and transcriptional activity in cells (Keller et al., 2001; Keller and Lu, 2002). Moreover, it has been described that CK2 is implicated in the response to UV irradiation-induced DNA damage, regulating p53 tumor suppressor protein functions through phosphorylation of Ser392 in p53 (Cox and Meek, 2010). In our excitotoxic context, we have described that AMPA triggers the molecular interaction between CK2 and p53, induces the translocation of p53 into the nucleus and that CK2 inhibitor reduces these effects (Figure 7). So, we were also trying to detect p-p53 (Ser392) in oligodendrocytes under excitotoxicity and a putative link between CK2 and p-p53 (Ser392) in this context. However, we have not observed p53 phosphorylation on Ser392 residue in oligodendrocytes after AMPA treatment (data not shown), so that p-p53 (Ser392) may in fact distinguish AMPA excitotoxicity from other stimuli

that have been described as having p53 activation through phosphorylation of Ser392.

The signaling described here raises the question of how a kinase like CK2, *a priori* prosurvival, may contribute to apoptotic program triggered by AMPA excitotoxic insult in oligodendrocytes. In this regard, JNK has been proposed as mediator of CK2 proapoptotic activity (Min et al., 2003), however the molecular mechanism through which CK2 can connect with JNK/p38 apoptotic pathway, and even with ASK1, under AMPA excitotoxic conditions needs to be explored in more detail. We hypothesize that CK2 is activated during early stages of apoptosis modulating a signaling mechanism with a dual action (anti or pro-apoptotic), which is able to influence a hypothetical ASK1/JNK/p38 axis. The UPR and, specifically, the IRE1 α pathway, could be the link between CK2 and pro-apoptotic JNK/p38 activation.

CK2 is also a regulator of the inflammatory response (Singh and Ramji, 2008), an intrinsic process that underlies many neurodegenerative diseases. Specifically, CK2 modulates neuroinflammatory events characteristic of Alzheimer's disease (Rosenberger et al., 2016) and experimental autoimmune encephalomyelitis (Axtell et al., 2006; Sestero et al., 2012; Gibson et al., 2017). Our results indicate that CK2 could be a therapeutic target not only restricted to the inflammatory process but also in relation to apoptotic program that triggers oligodendrocyte death in MS.

In summary, the findings reported here indicate that CK2 inhibition exerts oligoprotective effects from excitotoxic conditions induced by moderate activation of AMPA receptors, as it reduces ROS production and loss in mitochondrial potential. In turn, this cytoprotective effect of CK2 was mediated by a decrease in pro-apoptotic activation of JNK/p38/p53 signaling axis induced by AMPA receptors stimulation. We propose that CK2 inhibition is a promising target to protect oligodendrocytes from AMPA induced excitotoxic insults with potential implications for the treatment of demyelinating pathologies, especially MS disease.

REFERENCES

- Ahmad, K. A., Wang, G., Unger, G., Slaton, J., and Ahmed, K. (2008). Protein kinase CK2—a key suppressor of apoptosis. *Adv. Enzyme Regul.* 48, 179–187. doi: 10.1016/j.advenzreg.2008.04.002
- Allende-Vega, N., Dayal, S., Agarwala, U., Sparks, A., Bourdon, J. C., and Saville, M. K. (2013). p53 is activated in response to disruption of the pre-mRNA splicing machinery. *Oncogene* 32, 1–14. doi: 10.1038/onc.2012.38
- Antony, M. L., Kim, S. H., and Singh, S. V. (2012). Critical role of p53 upregulated modulator of apoptosis in benzyl isothiocyanate-induced apoptotic cell death. *PLoS One* 7:e32267. doi: 10.1371/journal.pone.0032267
- Atlante, A., Calissano, P., Bobba, A., Giannattasio, S., Marra, E., and Passarella, S. (2001). Glutamate neurotoxicity, oxidative stress and mitochondria. *FEBS Lett.* 497, 1–5. doi: 10.1016/s0014-5793(01)02437-1
- Axtell, R. C., Xu, L., Barnum, S. R., and Raman, C. (2006). CD5-CK2 binding/activation-deficient mice are resistant to experimental autoimmune encephalomyelitis: protection is associated with diminished populations of IL-17-expressing T cells in the central nervous system. *J. Immunol.* 177, 8542–8549. doi: 10.4049/jimmunol.177.12.8542
- Azim, K., and Butt, A. M. (2011). GSK3 β negatively regulates oligodendrocyte differentiation and myelination *in vivo*. *Glia* 59, 540–553. doi: 10.1002/glia.21122

AUTHOR CONTRIBUTIONS

MC-A, CM and MS-G conceived and designed the experiments and analyzed data. MC-A was involved in all experiments. MS participated in experiments with optic nerves of transgenic mice, their quantification and analysis of data. AM and SM took part in qPCR and subsequent analysis. AR, FL and JZ helped in the *in vitro* kinase assays and gene silencing experiments and interpreted the results. MS, FP-C and MS-G performed immunocytochemical analysis. MC-A, CM and MS-G prepared and wrote the manuscript and all authors provided critical feedback on the manuscript drafting and approved the final version to be published.

FUNDING

This study was supported by Centro de Investigación en Red de Enfermedades Neurodegenerativas (CIBERNED) and by grants from the Ministerio de Economía y Competitividad, Gobierno de España (Ministry of Economy, Industry and Competitiveness, Government of Spain; SAF2013-45084-R and SAF2016-75292-R to CM) and Ekonomiaren Garapen eta Lehiakortasun Saila, Eusko Jaurlaritza (Department of Economic Development and Competitiveness, Basque Government; IT702-13 to CM). MC-A and MS were predoctoral fellow from the Ministerio de Economía y Competitividad (BES-2011-047822 and BES-2014-070512, respectively).

ACKNOWLEDGMENTS

We thank Dr. F. Kirchhoff for generously providing us with PLP-DsRed mice. The expert technical assistance of Saioa Marcos, Juan Carlos Chara and Hazel Gómez, and support provided by SGIker of the Universidad del País Vasco (Animal Unit and Analytical and High-Resolution Microscopy in Biomedicine) is gratefully acknowledged.

- Bernal-Chico, A., Canedo, M., Manterola, A., Victoria Sánchez-Gómez, M., Pérez-Samartín, A., Rodríguez-Puertas, R., et al. (2015). Blockade of monoacylglycerol lipase inhibits oligodendrocyte excitotoxicity and prevents demyelination *in vivo*. *Glia* 63, 163–176. doi: 10.1002/glia.22742
- Bolton, C., and Paul, C. (2006). Glutamate receptors in neuroinflammatory demyelinating disease. *Mediators Inflamm.* 2:93684. doi: 10.1155/mi/2006/93684
- Cargnello, M., and Roux, P. P. (2012). Activation and function of the MAPKs and their substrates, the MAPK-activated protein kinases. *Microbiol. Mol. Biol. Rev.* 75, 50–83. doi: 10.1128/MMBR.00031-10
- Chen, Y., Balasubramanian, V., Peng, J., Hurlock, E. C., Tallquist, M., Li, J., et al. (2007). Isolation and culture of rat and mouse oligodendrocyte precursor cells. *Nat. Protoc.* 2, 1044–1051. doi: 10.1038/nprot.2007.149
- Choi, D. W. (1988). Glutamate neurotoxicity and diseases of the nervous system. *Neuron* 1, 623–634. doi: 10.1016/0896-6273(88)90162-6
- Choi, H. J., Kang, K. S., Fukui, M., and Zhu, B. T. (2011). Critical role of the JNK-p53-GADD45 α apoptotic cascade in mediating oxidative cytotoxicity in hippocampal neurons. *Br. J. Pharmacol.* 162, 175–192. doi: 10.1111/j.1476-5381.2010.01041.x
- Cox, M. L., and Meek, D. W. (2010). Phosphorylation of serine 392 in p53 is a common and integral event during p53 induction by diverse stimuli. *Cell. Signal.* 22, 564–571. doi: 10.1016/j.cellsig.2009.11.014

- Dhanasekaran, D. N., and Reddy, E. P. (2008). JNK signaling in apoptosis. *Oncogene* 27, 6245–6251. doi: 10.1038/onc.2008.301
- Domercq, M., Pérez-Samartín, A., Aparicio, D., Alberdi, E., Pampliega, O., and Matute, C. (2010). P2X7 receptors mediate ischemic damage to oligodendrocytes. *Glia* 58, 730–740. doi: 10.1002/glia.20958
- Domercq, M., Sánchez-Gómez, M. V., Sherwin, C., Etxebarria, E., Fern, R., and Matute, C. (2007). System x_c^- and glutamate transporter inhibition mediates microglial toxicity to oligodendrocytes. *J. Immunol.* 178, 6549–6556. doi: 10.4049/jimmunol.178.10.6549
- Fausti, F., Di Agostino, S., Cioce, M., Bielli, P., Sette, C., Pandolfi, P. P., et al. (2013). ATM kinase enables the functional axis of YAP, PML and p53 to ameliorate loss of Werner protein-mediated oncogenic senescence. *Cell Death Differ.* 20, 1498–1509. doi: 10.1038/cdd.2013.101
- Finlan, L. E., Nenutil, R., Ibbotson, S. H., Vojtesek, B., and Hupp, T. R. (2006). CK2-site phosphorylation of p53 is induced in $\Delta Np63$ expressing basal stem cells in UVB irradiated human skin. *Cell Cycle* 5, 2489–2494. doi: 10.4161/cc.5.21.3393
- Galluzzi, L., Blomgren, K., and Kroemer, G. (2009). Mitochondrial membrane permeabilization in neuronal injury. *Nat. Rev. Neurosci.* 10, 481–494. doi: 10.1038/nrn2665
- Gibson, S. A., Yang, W., Yan, Z., Liu, Y., Rowse, A. L., Weinmann, A. S., et al. (2017). Protein Kinase CK2 controls the fate between Th17 cell and regulatory T cell differentiation. *J. Immunol.* 198, 4244–4254. doi: 10.4049/jimmunol.1601912
- Gong, X., Liu, A., Ming, X., Deng, P., and Jiang, Y. (2010). UV-induced interaction between p38 MAPK and p53 serves as a molecular switch in determining cell fate. *FEBS Lett.* 584, 4711–4716. doi: 10.1016/j.febslet.2010.10.057
- González-Fernández, E., Sánchez-Gómez, M. V., Pérez-Samartín, A., Arellano, R. O., and Matute, C. (2014). A3 Adenosine receptors mediate oligodendrocyte death and ischemic damage to optic nerve. *Glia* 62, 199–216. doi: 10.1002/glia.22599
- Gray, G. K., McFarland, B. C., Rowse, A. L., Gibson, S. A., and Benveniste, E. N. (2014). Therapeutic CK2 inhibition attenuates diverse prosurvival signaling cascades and decreases cell viability in human breast cancer cells. *Oncotarget* 5, 6484–6496. doi: 10.18632/oncotarget.2248
- Guo, X., Harada, C., Namekata, K., Matsuzawa, A., Camps, M., Ji, H., et al. (2010). Regulation of the severity of neuroinflammation and demyelination by TLR-ASK1-p38 pathway. *EMBO Mol. Med.* 2, 504–515. doi: 10.1002/emmm.201000103
- Hanif, I. M., Shazib, M. A., Ahmad, K. A., and Pervaiz, S. (2010). Casein Kinase II: an attractive target for anti-cancer drug design. *Int. J. Biochem. Cell Biol.* 42, 1602–1605. doi: 10.1016/j.biocel.2010.06.010
- Hilgard, P., Czaja, M. J., Gerken, G., and Stockert, R. J. (2004). Proapoptotic function of protein kinase CK2 α is mediated by a JNK signaling cascade. *Am. J. Physiol. Gastrointest. Liver Physiol.* 287, 192–201. doi: 10.1152/ajpgi.00507.2003
- Hirrlinger, P. G., Scheller, A., Braun, C., Quintela-Schneider, M., Fuss, B., Hirrlinger, J., et al. (2005). Expression of reef coral fluorescent proteins in the central nervous system of transgenic mice. *Mol. Cell. Neurosci.* 30, 291–303. doi: 10.1016/j.mcn.2005.08.011
- Jiang, G., Wu, H., Hu, Y., Li, J., and Li, Q. (2014). Gastrin inhibits glutamate-induced apoptosis of PC12 cells via inhibition of CaMKII/ASK-1/p38 MAPK/p53 signaling cascade. *Cell. Mol. Neurobiol.* 34, 591–602. doi: 10.1007/s10571-014-0043-z
- Jin, L., Li, C., Xu, Y., Wang, L., Liu, J., Wang, D., et al. (2013). Epigallocatechin gallate promotes p53 accumulation and activity via the inhibition of MDM2-mediated p53 ubiquitination in human lung cancer cells. *Oncol. Rep.* 29, 1983–1990. doi: 10.3892/or.2013.2343
- Jones, R. G., Plas, D. R., Kubek, S., Buzzai, M., Mu, J., Xu, Y., et al. (2005). AMP-activated protein kinase induces a p53-dependent metabolic checkpoint. *Mol. Cell* 18, 283–293. doi: 10.1016/j.molcel.2005.03.027
- Ka, S. O., Hwang, H. P., Jang, J. H., Hyuk Bang, I., Bae, U. J., Yu, H. C., et al. (2015). The protein kinase 2 inhibitor tetrabromobenzotriazole protects against renal ischemia reperfusion injury. *Sci. Rep.* 5:14816. doi: 10.1038/srep14816
- Keller, D. M., and Lu, H. (2002). p53 serine 392 phosphorylation increases after UV through induction of the assembly of the CK2.hSPT16.SSRP1 complex. *J. Biol. Chem.* 277, 50206–50213. doi: 10.1074/jbc.M209820200
- Keller, D. M., Zeng, X., Wang, Y., Zhang, Q. H., Kapoor, M., Shu, H., et al. (2001). A DNA damage-induced p53 serine 392 kinase complex contains CK2, hSpt16, and SSRP1. *Mol. Cell* 7, 283–292. doi: 10.1016/s1097-2765(01)00176-9
- Kim, H., Tu, H. C., Takeuchi, O., Jeffers, J. R., Zambetti, G. P., Hsieh, J. J., et al. (2009). Stepwise activation of Bax and Bak by t-bid, BIM, and PUMA initiates mitochondrial apoptosis. *Mol. Cell* 36, 487–499. doi: 10.1016/j.molcel.2009.09.030
- Lee, J. M., Zipfel, G. J., and Choi, D. W. (1999). The changing landscape of ischaemic brain injury mechanisms. *Nature* 399, A7–A14. doi: 10.1038/399a007
- Li, M., Fang, X., Baker, D. J., Guo, L., Gao, X., Wei, Z., et al. (2010). The ATM-p53 pathway suppresses aneuploidy-induced tumorigenesis. *Proc. Natl. Acad. Sci. U S A* 107, 14188–14193. doi: 10.1073/pnas.1005960107
- Lipton, S. A., and Rosenberg, P. A. (1994). Excitatory amino acids as a final common pathway for neurologic disorders. *N. Engl. J. Med.* 330, 613–622. doi: 10.1056/nejm199403033300907
- Litchfield, D. W. (2003). Protein kinase CK2: structure, regulation and role in cellular decisions of life and death. *Biochem. J.* 369, 1–15. doi: 10.1042/bj20021469
- Loughery, J., Cox, M., Smith, L. M., and Meek, D. W. (2014). Critical role for p53-serine 15 phosphorylation in stimulating transactivation at p53-responsive promoters. *Nucleic Acids Res.* 42, 7666–7680. doi: 10.1093/nar/gku501
- Loughery, J., and Meek, D. (2013). Switching on p53: an essential role for protein phosphorylation? *Biodiscovery* 8:1. doi: 10.7750/biodiscovery.2013.8.1
- Manni, S., Brancalion, A., Tubi, L. Q., Colpo, A., Pavan, L., Cabrelle, A., et al. (2012). Protein kinase CK2 protects multiple myeloma cells from ER stress-induced apoptosis and from the cytotoxic effect of HSP90 inhibition through regulation of the unfolded protein response. *Clin. Cancer Res.* 18, 1888–1900. doi: 10.1158/1078-0432.ccr-11-1789
- Martínez-Hoyer, S., Aranguren-Ibáñez, A., García-García, J., Serrano-Candelas, E., Vilardell, J., Nunes, V., et al. (2013). Protein kinase CK2-dependent phosphorylation of the human regulators of calcineurin reveals a novel mechanism regulating the calcineurin-NFATc signaling pathway. *Biochim. Biophys. Acta* 1833, 2311–2321. doi: 10.1016/j.bbamcr.2013.05.021
- Mato, S., Sánchez-Gómez, M. V., Bernal-Chico, A., and Matute, C. (2013). Cytosolic zinc accumulation contributes to excitotoxic oligodendroglial death. *Glia* 61, 750–764. doi: 10.1002/glia.22470
- Matute, C. (2011). Glutamate and ATP signalling in white matter pathology. *J. Anat.* 219, 53–64. doi: 10.1111/j.1469-7580.2010.01339.x
- Matute, C., Alberdi, E., Domercq, M., Pérez-Cerdá, F., Pérez-Samartín, A., and Sánchez-Gómez, M. V. (2001). The link between excitotoxic oligodendroglial death and demyelinating diseases. *Trends Neurosci.* 24, 224–230. doi: 10.1016/s0166-2236(00)01746-x
- Matute, C., Sánchez Gómez, M. V., Martínez-Millán, L., and Mileli, R. (1997). Glutamate receptor-mediated toxicity in optic nerve oligodendrocytes. *Proc. Natl. Acad. Sci. U S A* 94, 8830–8835. doi: 10.1073/pnas.94.16.8830
- Matute, C., Torre, I., Pérez-Cerdá, F., Pérez-Samartín, A., Alberdi, E., Etxebarria, E., et al. (2007). P2X7 receptor blockade prevents ATP excitotoxicity in oligodendrocytes and ameliorates experimental autoimmune encephalomyelitis. *J. Neurosci.* 27, 9525–9533. doi: 10.1523/JNEUROSCI.0579-07.2007
- McCarthy, K. D., and de Vellis, J. (1980). Preparation of separate astroglial and oligodendroglial cell cultures from rat cerebral tissue. *J. Cell Biol.* 85, 890–902. doi: 10.1083/jcb.85.3.890
- McDonald, J. W., Althomsons, S. P., Hyrc, K. L., Choi, D. W., and Goldberg, M. P. (1998). Oligodendrocytes from forebrain are highly vulnerable to AMPA/kainate receptor-mediated excitotoxicity. *Nat. Med.* 4, 291–297. doi: 10.1038/nm0398-291
- Meek, D. W. (2009). Tumour suppression by p53: a role for the DNA damage response? *Nat. Rev. Cancer* 9, 714–723. doi: 10.1038/nrc2716
- Meek, D. W., and Cox, M. (2011). Induction and activation of the p53 pathway: a role for the protein kinase CK2? *Mol. Cell. Biochem.* 356, 133–138. doi: 10.1007/s11010-011-0966-3
- Meggio, F., and Pinna, L. A. (2003). One-thousand-and-one substrates of protein kinase CK2? *FASEB J.* 17, 349–368. doi: 10.1096/fj.02-0473rev

- Mier-Aguilar, C. A., Cashman, K. S., Raman, C., and Soldevila, C. (2016). CD5-CK2 signaling modulates Erk activation and thymocyte survival. *PLoS One* 11:e0168155. doi: 10.1371/journal.pone.0168155
- Min, Y. K., Park, J. H., Chong, S. A., Kim, Y. S., Ahn, Y. S., Seo, J. T., et al. (2003). Pyrrolidine dithiocarbamate-induced neuronal cell death is mediated by Akt, casein kinase 2, c-Jun N-terminal kinase, and I κ B kinase in embryonic hippocampal progenitor cells. *J. Neurosci. Res.* 71, 689–700. doi: 10.1002/jnr.10520
- Nieminen, A. I., Eskelinen, V. M., Haikala, H. M., Tervonen, T. A., Yan, Y., Partanen, J. I., et al. (2013). Myc-induced AMPK-phospho p53 pathway activates Bak to sensitize mitochondrial apoptosis. *Proc. Natl. Acad. Sci. U S A* 110, e1839–1848. doi: 10.1073/pnas.1208530110
- Nijboer, C. H., Heijnen, C. J., van der Kooij, M. A., Zijlstra, J., van Velthoven, C. T., Culumsee, C., et al. (2011). Targeting the p53 pathway to protect the neonatal ischemic brain. *Ann. Neurol.* 70, 255–264. doi: 10.1002/ana.22413
- Pampliega, O., Domercq, M., Soria, F. N., Villoslada, P., Rodríguez-Antigüedad, A., and Matute, C. (2011). Increased expression of cystine/glutamate antiporter in multiple sclerosis. *J. Neuroinflammation* 8:63. doi: 10.1186/1742-2094-8-63
- Park, B. S., Song, Y. S., Yee, S. B., Lee, B. G., Seo, S. Y., Park, Y. C., et al. (2005). Phospho-ser 15-p53 translocates into mitochondria and interacts with Bcl-2 and Bcl-xL in eugenol-induced apoptosis. *Apoptosis* 10, 193–200. doi: 10.1007/s10495-005-6074-7
- Pierre, F., Chua, P. C., O'Brien, S. E., Siddiqui-Jain, A., Bourbon, P., Haddach, M., et al. (2011). Pre-clinical characterization of CX-4945, a potent and selective small molecule inhibitor of CK2 for the treatment of cancer. *Mol. Cell. Biochem.* 356, 37–43. doi: 10.1007/s11010-011-0956-5
- Poole, A., Poore, T., Bandhakavi, S., McCann, R. O., Hanna, D. E., and Glover, C. V. (2005). A global view of CK2 function and regulation. *Mol. Cell. Biochem.* 274, 163–170. doi: 10.1007/s11010-005-2945-z
- Rao, F., Cha, J., Xu, J., Xu, R., Vandiver, M. S., Tyagi, R., et al. (2014). Inositol pyrophosphates mediate the DNA-PK/ATM-p53 cell death pathway by regulating CK2 phosphorylation of Tti1/Tel2. *Mol. Cell* 54, 119–132. doi: 10.1016/j.molcel.2014.02.020
- Rosenberger, A. F., Morrema, T. H., Gerritsen, W. H., van Haastert, E. S., Snkhchyan, H., Hillhorst, R., et al. (2016). Increased occurrence of protein kinase CK2 in astrocytes in Alzheimer's disease pathology. *J. Neuroinflammation* 13:4. doi: 10.1186/s12974-015-0470-x
- Saha, M. N., Jiang, H., Yang, Y., Zhu, X., Wang, X., Schimmer, A. D., et al. (2012). Targeting p53 via JNK pathway: a novel role of RITA for apoptotic signaling in multiple myeloma. *PLoS One* 7:e30215. doi: 10.1371/journal.pone.0030215
- Sánchez-Gómez, M. V., Alberdi, E., Ibarretxe, G., Torre, I., and Matute, C. (2003). Caspase-dependent and caspase-independent oligodendrocyte death mediated by AMPA and kainate receptors. *J. Neurosci.* 23, 9519–9528. doi: 10.1523/JNEUROSCI.23-29-09519.2003
- Sánchez-Gómez, M. V., Alberdi, E., Pérez-Navarro, E., Alberch, J., and Matute, C. (2011). Bax and calpain mediate excitotoxic oligodendrocyte death induced by activation of both AMPA and kainate receptors. *J. Neurosci.* 31, 2996–3006. doi: 10.1523/JNEUROSCI.5578-10.2011
- Sánchez-Gómez, M. V., and Matute, C. (1999). AMPA and kainate receptors each mediate excitotoxicity in oligodendroglial cultures. *Neurobiol. Dis.* 6, 475–485. doi: 10.1006/nbdi.1999.0264
- Sayed, M., Pelech, S., Wong, C., Marotta, A., and Salh, B. (2001). Protein kinase CK2 is involved in G2 arrest and apoptosis following spindle damage in epithelial cells. *Oncogene* 20, 6994–7005. doi: 10.1038/sj.onc.1204894
- Sestero, C. M., McGuire, D. J., De Sarno, P., Brantley, E. C., Soldevila, G., Axtell, R. C., et al. (2012). CD5-dependent CK2 activation pathway regulates threshold for T cell anergy. *J. Immunol.* 189, 2918–2930. doi: 10.4049/jimmunol.1200065
- Shah, S. A., Lee, H. Y., Bressan, R. A., Yun, D. J., and Kim, M. O. (2014). Novel osmotin attenuates glutamate-induced synaptic dysfunction and neurodegeneration via the JNK/PI3K/Akt pathway in postnatal rat brain. *Cell Death Dis.* 5:e1026. doi: 10.1038/cddis.2013.538
- Shi, Y., Nikulenkov, F., Zawacka-Pankau, J., Li, H., Gabdoulina, R., Xu, J., et al. (2014). ROS-dependent activation of JNK converts p53 into an efficient inhibitor of oncogenes leading to robust apoptosis. *Cell Death Differ.* 21, 612–623. doi: 10.1038/cdd.2013.186
- Simonishvili, S., Jain, M. R., Li, H., Levison, S. W., and Wood, T. L. (2013). Identification of Bax-interacting proteins in oligodendrocyte progenitors during glutamate excitotoxicity and perinatal hypoxia-ischemia. *ASN Neuro* 5:e00131. doi: 10.1042/an20130027
- Singh, N. N., and Ramji, D. P. (2008). Protein kinase CK2, an important regulator of the inflammatory response? *J. Mol. Med.* 86, 887–897. doi: 10.1007/s00109-008-0352-0
- Skulachev, V. P. (2006). Bioenergetic aspects of apoptosis, necrosis and mitoptosis. *Apoptosis* 11, 473–485. doi: 10.1007/s10495-006-5881-9
- Tilleux, S., and Hermans, E. (2007). Neuroinflammation and regulation of glial glutamate uptake in neurological disorders. *J. Neurosci. Res.* 85, 2059–2070. doi: 10.1002/jnr.21325
- Turowec, J. P., Duncan, J. S., French, A. C., Gyenis, L., St Denis, N. A., Vilks, G., et al. (2010). Protein kinase CK2 is a constitutively active enzyme that promotes cell survival: strategies to identify CK2 substrates and manipulate its activity in mammalian cells. *Meth. Enzymol.* 484, 471–493. doi: 10.1016/b978-0-12-381298-8.00023-x
- Ulges, A., Witsch, E. J., Pramanik, G., Klein, M., Birkner, K., Bühler, U., et al. (2016). Protein kinase CK2 governs the molecular decision between encephalitogenic TH17 cell and Treg cell development. *Proc. Natl. Acad. Sci. U S A* 113, 10145–10150. doi: 10.1073/pnas.1523869113
- Vilks, G., Saulnier, R. B., St. Pierre, R., and Litchfield, D. W. (1999). Inducible expression of protein kinase CK2 in mammalian cells. *J. Biol. Chem.* 274, 14406–14414. doi: 10.1074/jbc.274.20.14406
- Wang, J., Guo, W., Zhou, H., Luo, N., Nie, C., Zhao, X., et al. (2015). Mitochondrial p53 phosphorylation induces Bak-mediated and caspase-independent cell death. *Oncotarget* 6, 17192–17205. doi: 10.18632/oncotarget.3780
- Wang, L. W., Tu, Y. F., Huang, C. C., and Ho, C. J. (2012). JNK signaling is the shared pathway linking neuroinflammation, blood-brain barrier disruption and oligodendroglial apoptosis in the white matter injury of the immature brain. *J. Neuroinflammation* 9:175. doi: 10.1186/1742-2094-9-175
- Wu, G. S. (2004). The functional interactions between the p53 and MAPK signaling pathways. *Cancer Biol. Ther.* 3, 156–161. doi: 10.4161/cbt.3.2.614
- Yoshioka, A., Hardy, M., Younkin, D. P., Grinspan, J. B., Stern, J. L., and Pleasure, D. (1995). α -amino-3-hydroxy-5-methyl-4-isoxazolepropionate (AMPA) receptors mediate excitotoxicity in the oligodendroglial lineage. *J. Neurochem.* 64, 2442–2448. doi: 10.1046/j.1471-4159.1995.64062442.x
- Yu, J., Wang, Z., Kinzler, K. W., Vogelstein, B., and Zhang, L. (2003). PUMA mediates the apoptotic response to p53 in colorectal cancer cells. *Proc. Natl. Acad. Sci. U S A* 100, 1931–1936. doi: 10.1073/pnas.2627984100
- Zheng, Y., Qin, H., Frank, S. J., Deng, L., Litchfield, D. W., Tefferi, A., et al. (2011). A CK2-dependent mechanism for activation of the JAK-STAT signaling pathway. *Blood* 118, 156–166. doi: 10.1182/blood-2010-01-266320

Conflict of Interest Statement: The authors declare that the research was conducted in the absence of any commercial or financial relationships that could be construed as a potential conflict of interest.

Copyright © 2018 Canedo-Antelo, Serrano, Manterola, Ruiz, Llaverro, Mato, Zugaza, Pérez-Cerdá, Matute and Sánchez-Gómez. This is an open-access article distributed under the terms of the Creative Commons Attribution License (CC BY). The use, distribution or reproduction in other forums is permitted, provided the original author(s) and the copyright owner(s) are credited and that the original publication in this journal is cited, in accordance with accepted academic practice. No use, distribution or reproduction is permitted which does not comply with these terms.